

Heavenly Rooms

Design and fabrication of a sound absorptive panel composed of Helmholtz Resonators (HR) for improving the open office acoustics through reducing the annoyance caused by speech sounds

W COLLEGE OF BUILT ENVIRONMENTS
UNIVERSITY of WASHINGTON

nbbj **DMG** Design Machine Group

Student: Vidhya Rajendran
Faculty advisor: Tomás Méndez Echenagucia
Partner firm: NBBJ Seattle
Firm advisor: Ryan Mullenix

Acknowledgments

Doing this research was not easy for me but the journey was made enjoyable, thanks to all those individuals who helped me. I would like to thank my faculty advisor, Prof. Tomás Méndez Echenagucia, for his constant support, supervision, patience, and extensive knowledge in the field of acoustics. He pushed me in the right direction and made sure that I stayed on track throughout this research project. In addition, I would like to thank my firm advisor, Ryan Mullenix, who provided insights into workplace design and helped widen the scope of this research. He helped give a practical spin to this academic research project.

My sincere thanks go to Renée Cheng, the Dean of the College of Built Environments, for instituting the ARC program and for providing me with financial support which helped me spend more time on the research work. I would like to thank Jennifer E Davison, the Associate Director for students in the ARC program, for her constant guidance, support, and encouragement throughout the pilot year of this program. I really appreciate her help during the presentations.

I take this opportunity to express my gratitude to the NBBJ architecture firm in Seattle, a partner firm in this research project. I would like to thank Steve McConnell, Rich Dallam, and Nate Holland from NBBJ for their interest and valuable feedback on this project. Besides NBBJ, I would like to thank all the other partner firms for their time and efforts in progressing the student projects in the ARC program.

The experiments would not have been possible without the help from Prof. Andy Piacsek and Technician Peter Zencak from the Department of Physics in the Central Washington University. We collaboratively built the impedance tube setup for testing the panel samples. Their efforts, especially during the COVID pandemic time, is very appreciated. I would like to thank my professor, Roark Congdon, who lent me his 3D printer for fabricating the test samples during the lockdown. A huge thanks to my professors who run the fabrication lab - Jack Hunter and Kimo Griggs.

I would like to thank Arthur van der Harten, developer of the Pachyderm Acoustics plugin, for answering my questions on using his software. Last but not the least, I am grateful to my family for their moral support throughout my master's program.

Helmholtz Resonators in open office acoustics

Abstract

Acoustics is the only category in which a LEED-rated office building performs worse than a conventional building. The exposed hard surfaces and the lack of partitions cause easy propagation of conversational sounds between workstations in an open office. Research has shown that excess speech levels in the office cause disturbance to the occupants and can affect their work performance. Sound absorbers are relied upon for removing excess sound energy from spaces. But to address the absorption of speech sounds, porous absorbers are not efficient. Resonant absorbers, in particular Helmholtz Resonators, are effective at low frequencies and are applied to tackle the frequencies important for speech intelligibility in open offices.

This research focuses on designing a sound absorptive panel made of Helmholtz resonators of varying sizes that is effectual over the frequency spectrum important for speech sounds. The basics of Helmholtz resonators and their working principles are discussed. A space-efficient variant of the Helmholtz resonator that can achieve perfect absorption in the low frequencies is presented. An array of such resonators is implemented in the design of the resonator panel, as such a system can overcome the narrow performance quality of a unit resonator. Optimization algorithms are used in automating the design of the panel. The application of this panel in an open office improves its acoustic quality which are quantified through parameters like r_D , $D_{2,S}$, $L_{p,A,S,Am}$, and $L_{p,A,B}$. Ray tracing simulations are performed on three open office case studies to measure the acoustic improvements made by these panels. Among all the different locations of these panels, Pareto front sorting is applied to analyze the trade-offs for an optimal acoustic environment.

Contents

1	Introduction	1
1.1	Research questions and objectives	2
1.1.1	Aims and objectives	2
1.2	Research methods	3
2	Background	5
2.1	Performance rating of ‘Green’ buildings	5
2.2	Productivity metrics	5
2.3	Acoustics in Open offices	6
2.4	The low frequency problem	8
2.5	Sound absorption in open offices	9
3	Helmholtz Resonators	11
3.1	Working principles	11
3.2	Modifications to a Helmholtz resonator	12
4	Array of resonators	14
4.1	The coupling effect	14
4.2	Performance of an array of resonators	15
4.3	Semi-automated resonator array design	16
4.3.1	Enhancing the performance of the panel using additional resistance	16
4.4	Using the achieved absorption curve	17
4.5	The “best” panel	18
5	Open office acoustics	19
5.1	Single-number acoustic parameters for open offices	19
5.2	Room acoustic simulation	21
5.2.1	Office layouts	21
5.3	Study methodology	21
5.3.1	Background noise levels	22
5.3.2	Panel distribution in the open office	23
5.3.3	Panel heights	23
5.3.4	Multi-objective problem	24
5.4	Study 1 - Efficiency of the resonator panel	25
5.5	Study 2 - Benchmarking with conventional offices	27
5.6	Study 3 - Flat vs. Tilted HR panels	29
6	Open office case studies	31
6.1	Office layout 1	31
6.1.1	Baseline scenario	31

6.1.2	Improvements with HR panels	32
6.2	Office layout 2	35
6.2.1	Baseline scenario	36
6.2.2	Improvements with HR panels	37
6.3	Office layout 3	40
6.3.1	Baseline scenario	40
6.3.2	Improvements with HR panels	41
7	Application Considerations - Materials and Fabrication	45
7.1	Recycled objects as resonators	45
7.2	Acoustic metamaterials	46
8	Experimentation	48
8.1	Construction of the impedance tube	48
8.1.1	Source and its adapter	50
8.1.2	Microphones and their spacing	50
8.1.3	HR panel samples	51
8.1.4	Completed impedance tube setup	52
8.2	Experiment results	52
8.2.1	Experiment set 1	52
8.2.2	Experiment set 2	53
8.2.3	Experiment set 3	54
8.2.4	Experiment set 4	55
8.2.5	Limitations	56
9	Conclusions and discussion	57
9.1	Future work	58
10	Appendices	59
10.1	Appendix A - Helmholtz resonator's performance calculator	59
10.2	Appendix B - Semi-automated resonator array calculator	60
10.3	Appendix C - Open office acoustic simulations	61

1 Introduction

Over the last two decades, there has been a shift in office culture from private cubicles to open-plan offices. Open offices gained prominence for promoting worker collaboration and social interaction [Bradley, 2004]. They are economical and improve the mental health of the occupants. The lack of intervening partitions enhances most elements of workplace comfort - indoor air quality, natural lighting, and visual access to the outdoors. Unfortunately, this also enables unhindered sound propagation in open offices. The originating sound can travel longer distances within the office. Sound from human activities and speech can interfere with the cognitive abilities of the employees [Delle Macchie et al., 2018, Ebissou et al., 2015]. In open offices, the hard reflective surfaces and the insufficiency of sound barriers cause the distracting noises to affect many more people than in a conventional office setup [Hodgson, 2011, Lee and Kim, 2008].

Sound absorbent surfaces help to reduce the detrimental effects of noise in the space. But with the type of office furnishings and conventional ceiling absorbents, acoustic comfort is not attained in open offices [Delle Macchie et al., 2018]. Porous absorbers are commonly used for sound absorption in open offices. They are effective in absorbing mid to high frequency sound spectrum. This emphasis on damping the mid to high frequencies is because humans are more sensitive to frequencies above 500Hz, though our audible range is between 20Hz-20kHz, and we perceive them to be loud. Most activities, speech and mechanical noises contain energy in the whole sound spectrum. Damping the mid and high frequencies causes a concentration of low frequency sound in the space, which can be heard as a “hum”. Though low frequencies are not heard as a loud sound, they can cause annoyance and stress in people [Leventhall et al., 2004, Pierre Jr et al., 2004]. Long exposure to low frequency noise in the workplace adversely affects the employee’s concentration and work performance.

Unlike porous absorbers, resonant absorbers are effective in absorbing low frequencies. They attenuate the sound by the vibration motion of an air column that connects the environment having sound waves to an enclosed cavity of air [Cox and d’Antonio, 2016]. Helmholtz Resonators, a type of resonant absorber, are of particular interest in this research study. A Helmholtz Resonator with a specific geometrical construct can absorb a narrow range from the low frequency spectrum. Fortunately, many such constructs are possible and each resonator design can absorb different bandwidths from the low frequency spectrum. By combining different sized resonators into an array or panel, a large bandwidth could be absorbed, even larger than the sum of individual absorption bandwidths [Griffin et al., 2000]. This is made possible by their coupling effect. Such a panel can be hung from the ceiling or applied to wall surfaces in open offices to absorb and to obstruct the concentration of low frequencies.

The acoustic quality of the open office with ceiling-hung Helmholtz resonator panels fares better in comparison to offices without any low frequency absorbers. With this inclusion, the

reverberation time in each octave can be maintained within 1 second which averts the “hum”. Addressing the low frequency problem in open-plan offices can help improve the occupant satisfaction, and thereby the work productivity of the employees [Fuchs, 2013].

1.1 Research questions and objectives

Since the inception of open offices in the 1950s, the problem of providing a positive working environment has been a persistent challenge. The occupants in open offices show dissatisfaction and reduced work productivity [Delle Macchie et al., 2018]. In a research [Brennan et al., 2002] that tracked the satisfaction of the employees who were relocated from traditional offices to open offices, the results showed a decrease in occupant satisfaction. The dissatisfaction continued long after they were relocated and there was a lower perceived job performance. A majority of those complaints are targeted at the acoustical comfort present in the work areas. At the same time, open offices can offer economic and cultural incentives as indicated by the LEED rating system’s preference for open offices. The acoustic challenge in open offices has led to the following research questions.

Main research questions - It is cited that employees are distracted by conversational noises in the open office [Delle Macchie et al., 2018, Ebissou et al., 2015]. So, how can an absorber be designed to specifically attenuate the frequencies important for speech intelligibility in open offices? Is it possible to improve the open office acoustics with such an absorber?

Secondary questions -

- Can Helmholtz resonators be used to address the low frequency noise problem?
- How to design an absorber composed of Helmholtz resonators? Would it be efficient in attenuating the sound frequencies important for speech intelligibility?
- What is the impact of such an absorber in open office acoustics?
- How can this absorber be architecturally integrated into the design?
- How can this absorber be fabricated? What materials can be used for better results, and what are the constraints involved in its fabrication?

1.1.1 Aims and objectives

The goal of this research is to investigate the application of Helmholtz resonators to improve open office acoustics issues. Helmholtz resonators are used as acoustic liners for reducing noise in airplanes and automobiles. In architecture, they are used for removing room modes or standing waves, especially in engine rooms or recording studios which produce the same frequency or bass frequencies sound throughout [Jordan, 1947]. Hence, these resonators are already proven to be good at attenuating low frequency noise. Through this research, the possibility of extending the application of Helmholtz resonators to a diffuse sound field is examined.

In open offices, a wide range of sound frequencies exists in a reverberant field. In such a case, the sound incident on the resonators could be from any direction. To address the broadband spectrum, a number of resonators working in different frequencies would have to be put together.

The main objective of this research is to design a broadband absorber composed of Helmholtz resonators of varying sizes to address the speech intelligibility complaints in open offices. The addition of porous materials to enhance the absorption capabilities of the resonator is avoided in this research considering the possibility of dust collection in the fibers. The ideal absorber would be simple, yet efficient, in improving the acoustical comfort in open offices.

1.2 Research methods

Work Scales	Models	Parameters	Performance
Helmholtz Resonator	→ Analytical	Geometry Fabrication	Absorption coefficient vs. Size and/or Material
Array of Resonators	→ Literature → Analytical → Experimental	Optimal Combination Fabrication	Bandwidth of noise absorption Absorption coefficient vs. Size / Cost / Build complexity
Room scale	→ Ray tracing	Panel Location Office layout	Spatial decay rate of speech Reverberation time Distraction distance Amount of absorptive surfaces

Figure 1: Work scales and its associated models, parameters, and performance criteria

The research is split into three work scales - individual resonators, an array of resonators in the form of a panel, and the application of the panels in open offices. Though these work scales are developed sequentially, the results from one work scale influence the design in the other scales. Experimental validation has been done for the array of resonators scale.

At the scale of the individual resonator, the goal is to design a unit resonator which maximizes the absorption performance within the desired spectrum of sound. Analytical models are used to predict the absorption performance of the resonator. While the analysis considered only the geometrical configuration of the resonator, design considerations include probable fabrication procedures. The resonator's performance is evaluated based on the trade-off between its sizing and its maximum absorption coefficient.

At the array of resonators scale, resonators of various geometries are packed together into a system. The coupling effect improves the overall performance of the system. To maximize this system's performance, the resonators' resonant frequencies are spaced out evenly within the bandwidth of interest. Analytical methods, as suggested by Kim [Kim, 2010], are employed in designing an absorptive panel within the desired bandwidth. Experiments were conducted on a few samples to validate the results from the analytical methods. The performance of the designed panels are ranked based on its bandwidth of absorption, its peak performance, and the complexity involved in fabricating the panel.

At the room-scale, the best panel sample is modeled into various open office layouts to test its efficacy in improving the acoustics of the space. Geometrical acoustic simulations are performed for this evaluation. Single-number acoustic values, as specified in the ISO 3382-3, are used for comparing the improvements induced by the resonator panels. Pareto front analysis is applied between the number of absorptive panels required (hence, the cost) to achieve good acoustics and the single-number acoustical ratings of their performance, for each office layout.

2 Background

2.1 Performance rating of ‘Green’ buildings

In open offices, the noise levels could reach up to 60 dB. Though open offices are designed to enhance the connectivity between teams and to reduce the maintenance costs, they lack in providing speech privacy and a quiet working environment. Center for Built Environment (CBE) at the University of California, Berkeley designed a web-based occupant satisfaction survey to gain insights into workplace productivity. The results from the survey of over 200 office buildings are given in figure 2. LEED-rating is used as a means to categorize the office buildings into ‘Green’ and ‘non-Green’ buildings.

Mean satisfaction score	Database buildings: all (non-green)	Database buildings: age<15 (non-green)	LEED-rated / green buildings
Office Layout	0.95	1.03	0.94
Office Furnishings *	0.84	1.03	1.26
Thermal Comfort *	-0.16	0.17	0.36
Air Quality * ^	0.21	0.52	1.14
Lighting	1.12	1.16	1.08
Acoustics	-0.20	-0.01	-0.27
Cleaning and Maint...*	0.91	1.15	1.48
Overall Workspace *	0.84	1.03	1.13
Overall Building *	0.93	1.14	1.47
Number of buildings	160	35	21

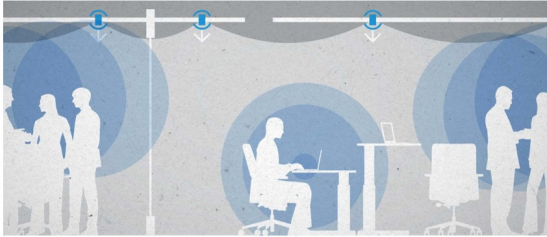


Figure 2: (Left) Satisfaction comparison across all CBE survey categories among three groups: database buildings, new database buildings, and LEED-rated/green buildings [Abbaszadeh et al., 2006]; (Right) Conversational sounds is the main source of distraction in open offices

Acoustics is the only category in which a LEED-rated office building performs worse than a conventional building [Abbaszadeh et al., 2006, Hodgson, 2011, Lee and Kim, 2008]. This aspect is very prominent in offices with low partition walls or open-plan offices than the offices with high screens. Employees in open offices are often disturbed by conversational sounds from neighboring areas. The hard exposed wall surfaces and the lack of sufficient partitions reflect the babble sounds within the open office. But more importantly, LEED “virtually ignores acoustics” [Hodgson, 2011]. Hence, sufficient attention is not paid towards acoustic comfort in the workplace environment.

2.2 Productivity metrics

CompTIA Cyberstates 2020 released the U.S. tech industry’s workforce and the total GDP generated in 2019. From this, it can be estimated that even a 1% decrease in employee productivity (which could be just about 5 minutes a day) could potentially cost the company almost \$1500 per employee per year.

Tech Industry (2019)

$$\frac{\$1.9 \text{ trillion (GDP in tech)}}{12.1 \text{ million workers}} = \$1,57,024/\text{tech worker}$$

1% reduction = **\$1570/employee**

Figure 3: Productivity metrics in the Tech industry section from 2019 [cyberstates.org, 2020]

2.3 Acoustics in Open offices

In open offices, the occupants are distracted by speech levels and activities occurring around them. A poor acoustic condition weakens their ability to concentrate and affects their work productivity [Ebissou et al., 2015]. A decrease in task performance is correlated with Speech Transmission Index (STI) (refer figure 4). The STI is a 0 to 1 index, that represents the “transmission quality of speech”, where 1 represents a perfectly speech-intelligible situation and 0 corresponds to a perfectly speech-private condition. In open offices, an STI value of 0.2 or less is required to maintain the occupant productivity levels [ISO 3382-3, 2012].

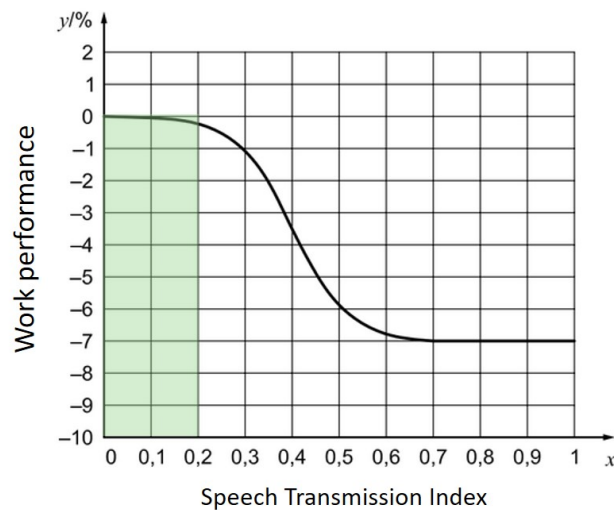


Figure 4: STI vs Task performance [ISO 3382-3, 2012]

Two kinds of sound levels contribute to the evaluation of STI - Conversational sound and background noise. While it is a common mistake to remove the background noise for better acoustic quality, the contrary is found to be true in offices [Rindel, 2018]. People find it comforting to work in the presence of mild background noise. This is because the background noise plays a masking role for the remote speech sounds. However, if its value is too high, it could affect the work performance. To achieve a STI value of 0.25, the speech and noise levels will

have to be maintained as shown in figure 5. The background noise levels will have to be slightly higher than the conversational or speech sound to effectively mask the speech and provide speech privacy.

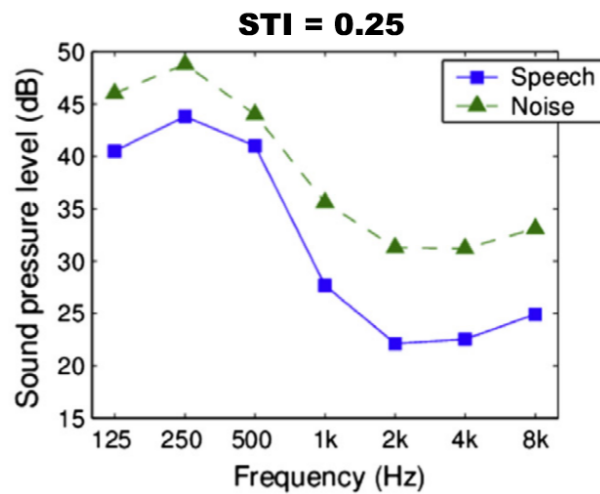


Figure 5: Sound levels for a STI value of 0.25 [Ebissou et al., 2015]

The typical speech level in an open office is depicted in figure 6. It is noticeable that the Intermediate Office Speech Level (IOSL) exceeds the required speech levels for an STI value of 0.25. And this excess sound is, mostly, concentrated in the low frequency range (up to 600 Hz). low frequency sound can be related to the sound from the left-hand keynotes on the piano. It is important to address the sound absorption of low frequencies to reduce the overall speech sounds in open offices. Tackling the speech sounds at their source helps in selectively attenuating them without completely removing the background noise. Removing the conversational sound adds a layer of speech privacy to the occupants, which is another prominent acoustics complaint.

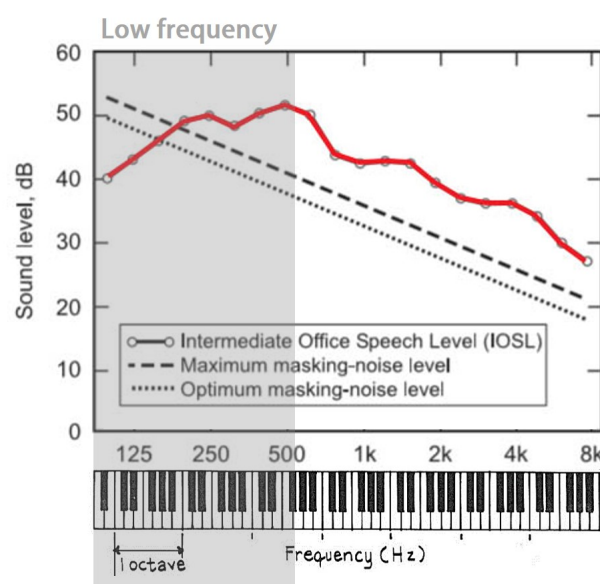


Figure 6: Speech spectrum in Open offices [Bradley, 2003]

2.4 The low frequency problem

One of the sources of low frequency noise in workplaces is from human speech. Human sentences are composed of vowels and consonants. The consonants carry the information content of speech while vowels carry the sound volume of speech. Mapping out the consonants and vowels on a frequency scale shows that consonants are largely clustered in mid to high frequencies while vowels occupy the lower frequencies [Davidsson, 2016]. As shown in figure 7, most of the spoken syllables fall in the low frequency spectrum and does contribute to the low frequency noise in open offices.

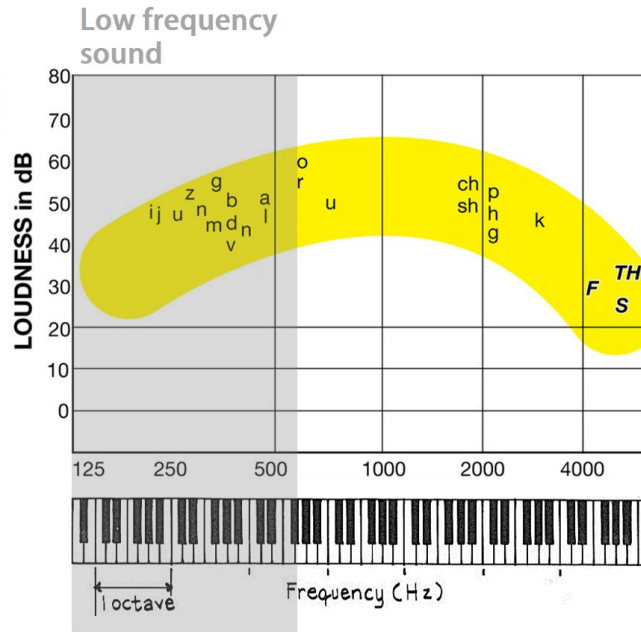


Figure 7: Mapping the spoken syllables on the frequency axis

The annoyance caused by low frequency sound is underestimated [Leventhall et al., 2004, Pierre Jr et al., 2004]. low frequency sound includes frequencies in the range 10Hz to 300Hz. Typically, A-weighting is used as a standard for measuring the loudness of sound. It factors in the sensitivity of human ears to the full audible range of frequencies (20Hz-20kHz). The A-weighting standard, though widely accepted and used in measuring noise levels, de-emphasizes the low frequency noise content [Pierre Jr et al., 2004]. Research studies have shown that low frequency noises, also known as the “hum”, are perceived by many as loud and annoying compared to other noises of the same SPL. But the A-weighting standard has reduced the attention placed on attenuating the low frequency noises. Unfortunately, low frequency noises can travel longer distances without losing much energy and they are attenuated less by walls and other structures.

Fuchs [Fuchs, 2013] rightly points at the low frequency problem, both in terms of measuring it and in attenuating it. Low frequency noise can amplify certain room modes, and this not only causes uneasiness but it also hinders the measurement of SPL at low frequencies. Noise

is best controlled when tackled at its source. But low frequency noises are difficult to control at their source and can bounce around the room without losing much of the energy. Even the partitions placed in the open offices don't contribute much in attenuating low frequencies. Edge diffraction allows for low frequencies to easily bend around tall partition walls or even the desk screens.

2.5 Sound absorption in open offices

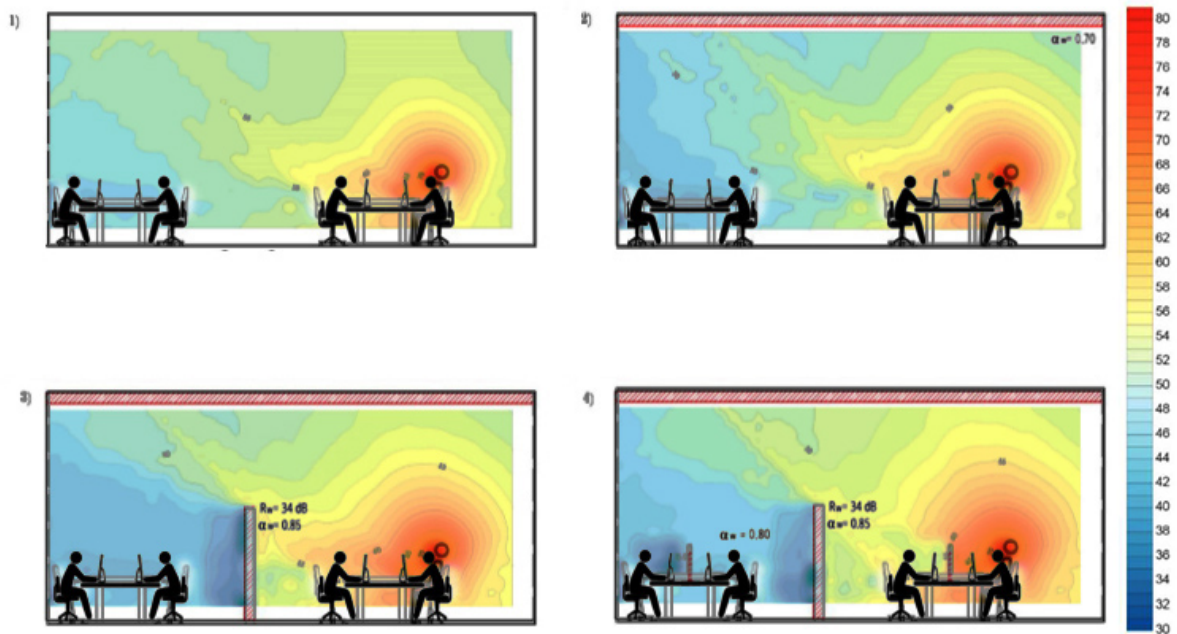


Figure 8: Sound absorption in open offices [Delle Macchie et al., 2018]

Typically, diffusive or rough surfaces are used to scatter the incident sound waves in open offices. But, this strategy only ensures that the sound does not concentrate in a particular zone. On the other hand, sound absorptive surfaces remove the excess sound energy from the space. Figure 8 shows a case-wise reduction in the sectional area affected by a speaker in an open office using sound absorbers. Use of absorptive material on the ceiling is very effective in impeding the sound transmission in open offices.

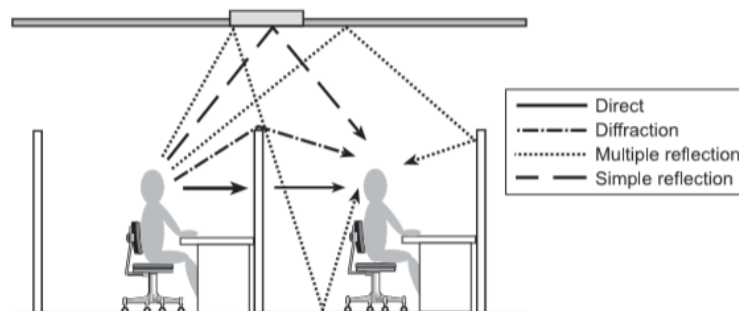


Figure 9: Sound path between workstations [Bradley, 2004]

Porous absorbers are commonly used as acoustic insulation in the walls, as they perform well in mid to high frequencies. But it is difficult to achieve low frequency sound absorption with porous absorbers due to the required thickness of the material; porous absorbers need to be at least a quarter wavelength thick for quality sound absorption. Also, within a space, absorbers are preferred at room boundaries and porous absorbers are not efficient at the boundaries where the wave velocity is low [Cox and d’Antonio, 2016]. Resonant absorbers, on the other hand, are very effective when placed at the room boundaries. They have their peak absorption in the low frequency, but unlike porous absorbers, the sound attenuation capacity is dependent on the dimensions of the structure rather than the material properties.

Membrane or panel absorbers and resonant absorbers are designed for trapping low frequencies (figure 10). Diaphragmatic absorber, a popular membrane absorber, is quite efficient in tackling frequencies as low as 50Hz but it needs a large cavity (200mm-300mm) for such low frequencies. Helmholtz resonators, a resonant absorber, is also a low frequency absorber and requires a deeper cavity for effective absorption. However, there have been recent developments in making them compact without compromising the performance. For instance, a sub-wavelength acoustic resonator, which is 3 or 4 times shorter, can achieve the same results as a traditional Helmholtz resonator [Yuan et al., 2019]. Also, resonant absorbers are considered as a “healthier” alternative to porous absorbers as they do not have any spongy components that may lead to dust collection. This also helps prevent mold formation in their pores.

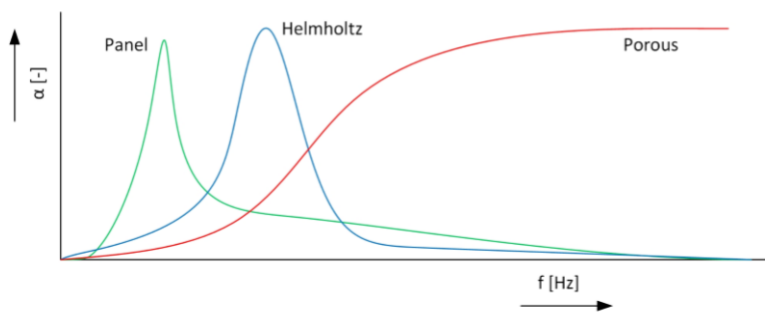


Figure 10: Performance of different sound absorbers [Gommer, 2016]

3 Helmholtz Resonators

Long before Helmholtz resonators evolved, the Greeks designed “vessels” to modify the acoustics in their theatres. Vitruvius, a great Roman architect, in his book, described the embedding of brass “vessels” in the reflective stone or marble walls of the theatre to improve the sound quality [Rindel, 2011]. In the 19th century, the German physicist Hermann von Helmholtz studied the phenomenon of air resonance in hollow spherical cavities with short and narrow necks. He used varying sizes of these resonators to study the frequencies in music, to amplify a particular frequency in a complex sound wave. His resonator design was later named after him. Now, several modifications have been made to the original design to make it more compact and efficient.

3.1 Working principles

Helmholtz resonators resemble an empty bottle with an open mouth. When sound waves pass over this opening, it vibrates the air column in the neck which converts sound energy into thermal losses. The plug of air in the neck acts as a vibrating mass against the spring provided by the air enclosed in the cavity. Damping is caused by viscous losses along the surface of the neck and radiation losses at the ends of the neck.

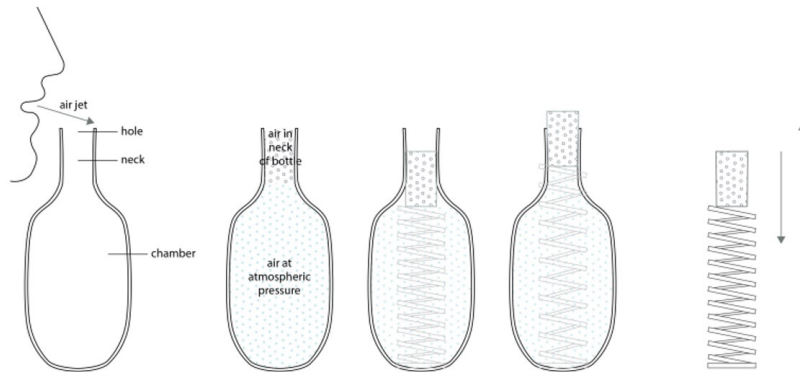


Figure 11: Working principle of a Helmholtz resonator

By changing the vibrating mass and the stiffness of the air spring, the resonant frequency of the device can be tuned, and it is at the resonant frequency that absorption is maximum. But their bandwidth of absorption is very narrow and limited. This drawback could be overcome by combining multiple Helmholtz resonators of varying geometries (or resonant frequencies) to achieve a broader bandwidth of absorption (refer figure 12). The resonant frequency is given by [Cox and d’Antonio, 2016]:

$$f_0 = \frac{c}{2\pi} \sqrt{\frac{S_n}{l'V_c}} \quad (3.1)$$

where S_n is the area of the neck opening ($S_n = \pi r^2$), r is the radius of the neck, l' is the corrected length of the neck, and V_c is the volume of the cavity.

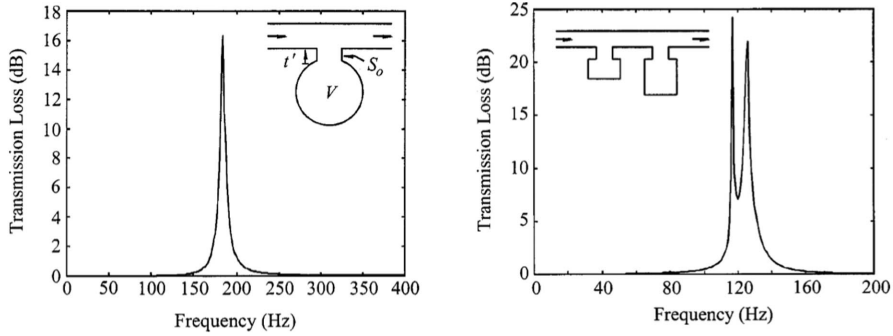


Figure 12: (Left) Sound absorption of a single resonator; (Right) Sound absorption of two resonators connected in series [Griffin et al., 2000]

3.2 Modifications to a Helmholtz resonator

This research only discusses concentric resonators, that have the center of the neck and the center of the cavity along the same axis. The resonators are considered to be loaded on a baffle to model a sound absorptive panel.

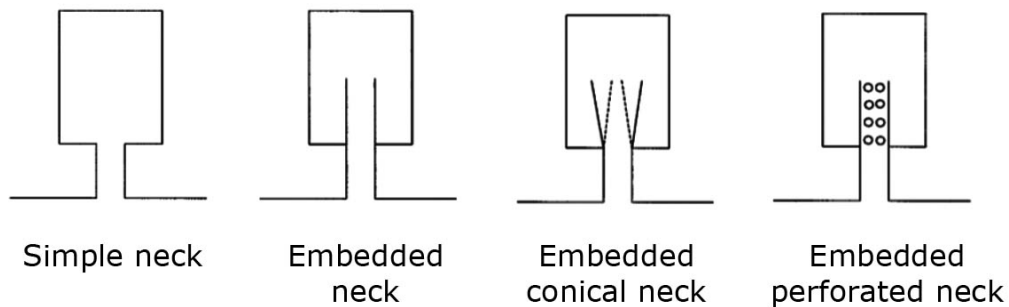


Figure 13: Modifications suggested by Selamet [Selamet and Lee, 2003]

A simple resonator design is a cylindrical cavity with a cylindrical neck. Modification to the cross-section of the cavity introduces a square cavity attached to a cylindrical neck. Such a design is space-efficient especially when multiple resonators are packed together into a panel. A square resonator with exact dimensions to that of the cylindrical resonator (the diameter of the cylindrical cavity equates to the edge length of the square cavity) has a lower resonant frequency and a better absorption peak value in the low frequencies.

Adaptation of the neck geometry of a simple resonator presents the embedded neck model. Instead of having the neck protrude outwards, having the neck immersed into the cavity's volume of the resonator saves space. This design shifts the performance peak to lower frequencies but maintains the peak absorption value. Another variant is developed by switching the cylindrical neck for a conical cross-section. This resonator shifts the resonant frequency higher with increasing taper length. Though it has a better absorption performance, its performance has a narrow bandwidth when compared to a simple resonator.

In this research, the embedded neck resonator is used as it is space-efficient and can achieve lower resonant frequencies compared to the simple resonator geometry. The embedded neck resonator model can easily be fabricated using 3D printing technology.

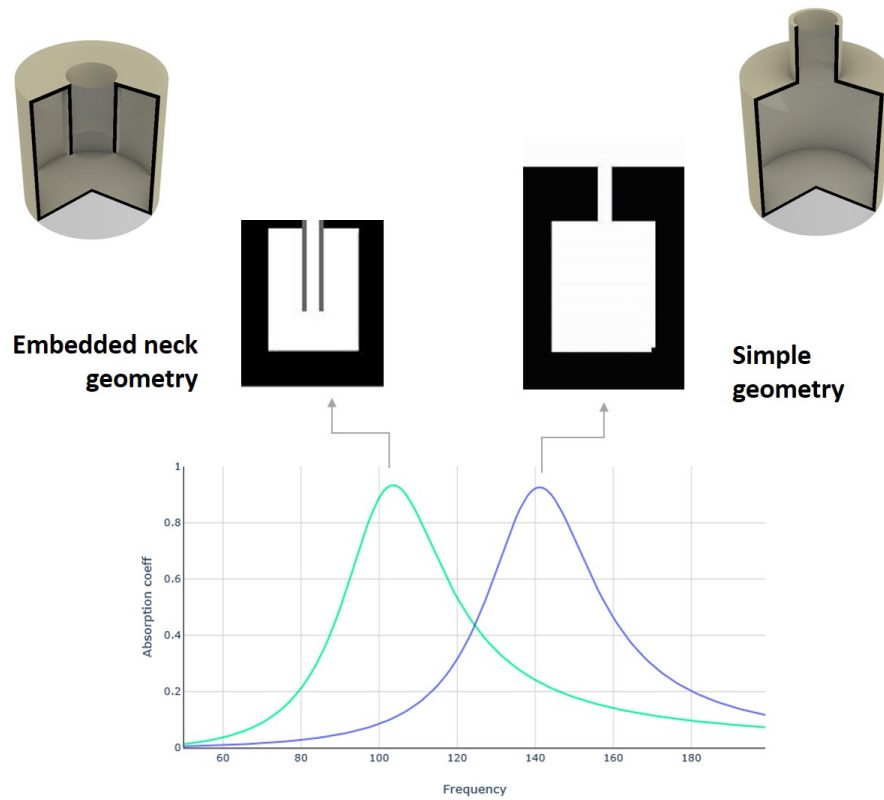


Figure 14: Comparison between the embedded neck and the simple geometry resonators

4 Array of resonators

A single resonator is not very effective in absorbing a wide spectrum of frequencies. As shown in figure 12, combining two or more dissimilar resonators broadens the bandwidth of absorption. When unit resonators are placed close to one another, they influence each other—the coupling effect. This interaction becomes weaker as the distance between the resonators increases [Johansson and Kleiner, 2001]. It is cited that resonators with similar resonant frequencies, when placed in close proximity, can maximize the absorption of the system compared to resonators with very dissimilar resonant frequencies [Van der Aa, 2012].

4.1 The coupling effect

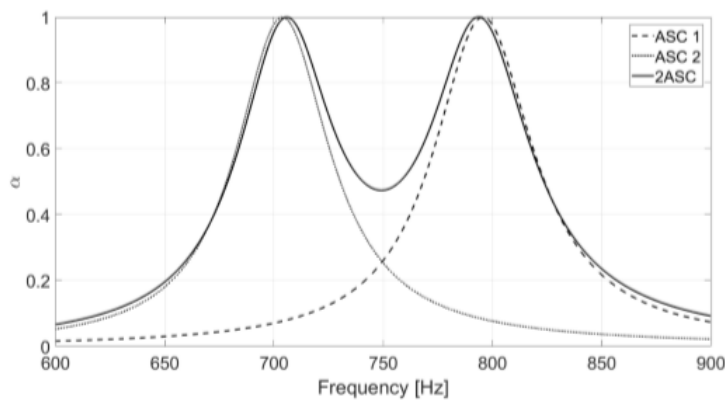
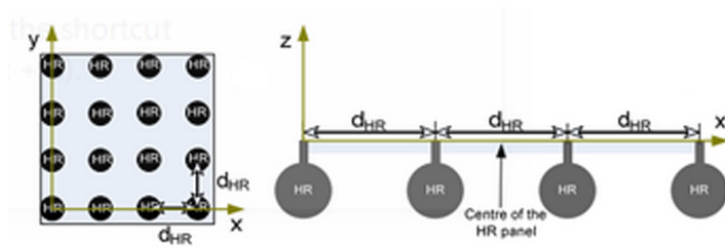


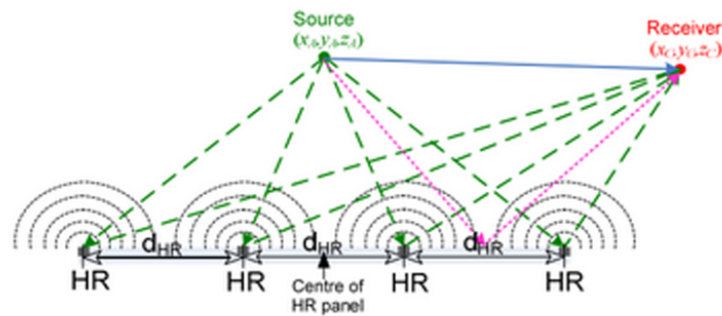
Figure 15: *Effect of mutual interaction between two resonators [Carvalho De Sousa et al., 2019]*

The coupling effect is depicted in figure 15. The bold line represents the absorption performance of the system of two different resonators placed next to each other and the other two lines are the individual performance of the resonators. The difference between the valley where the individual’s performances cross over and the trough in the system’s performance is caused by the interaction between the two resonators.

To account for this interaction in the absorption calculation, an additional term is added to the radiation impedance, known as mutual radiation impedance. The mass of air vibrating in the neck is modeled as a circular piston moving up and down. The movement expends radiation energy as shown in figure 16. When the source excites the resonators, the circular pistons are set in motion which produces radiation waves. The resonators in the vicinity of a radiating resonator face the additional radiation on top of the self radiation due to direct excitation by the source. This causes the mutual interaction effect observed in the graph (figure 15). As the resonators are moved away from each other, the impact of one’s radiation on another becomes weaker and their combined performance tapers.



Plan and section of the 4*4 panel



Working of the HR panel

Figure 16: Radiation energy from a Helmholtz resonator panel of 4*4 identical resonators [Polychronopoulos et al., 2014]

4.2 Performance of an array of resonators

The coupling effect is not just observed between two closely-placed resonators but can be observed between any number of resonators packed in an array. This beneficial interaction between the resonators depends on the neck area of the resonators and their distance from other resonators. For an array of 9 dissimilar resonators, whose individual performances are shown in figure 18, the mutual interaction between them improves the overall performance of the array rather than just a direct overall of the individual performances. Hence, with dissimilar resonators in the array, the absorption performance is broader and it overcomes the drawbacks of a unit resonator.

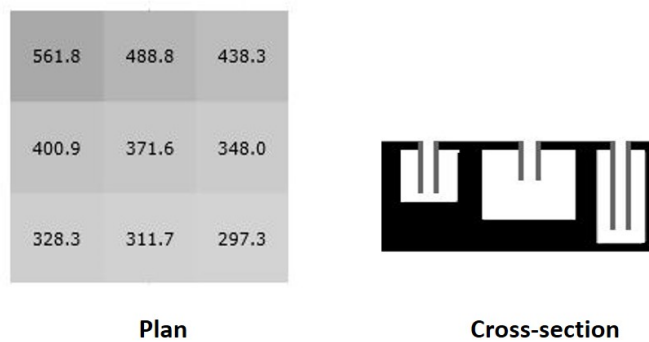


Figure 17: Plan (resonant frequencies depicted) and cross-section of a 3x3 array of dissimilar resonators (embedded neck geometry)

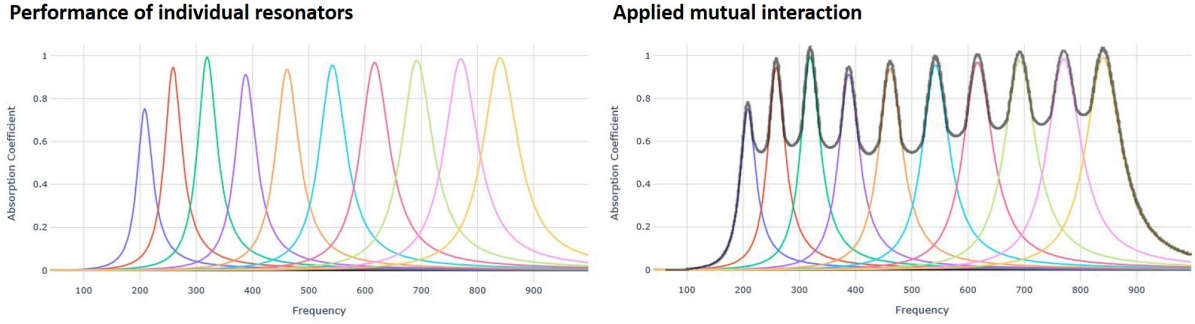


Figure 18: (Left) Performance of the individual resonators used in the 3×3 array; (Right) The black line depicts the applied mutual interaction between the resonators, and hence depicts the overall performance of the array

4.3 Semi-automated resonator array design

A simpler interface that requires minimum input from the users was engaged for designing an optimal performing panel. In this semi-automated approach, the frequency bandwidth of the panel's performance and the panel's depth are the variables that control the panel's design. Once given, the algorithm looks for possible resonator geometry combinations that could target the frequencies in the given bandwidth. This algorithm is based on the brute-force search which analyzes all possible combinations. Though multiple resonator constructs can have the same resonant frequency, the algorithm chooses one that maximizes the peak absorption performance. These resonators are arranged randomly in the panel since the radiation impedance method does not factor in the distribution pattern of the resonators. Appendix B shows the working of the interface which implements the above algorithm. Figure 20 shows the absorption performance of an optimal panel from a given set of inputs.

4.3.1 Enhancing the performance of the panel using additional resistance

The result achieved in figure 20 has prominent valleys in-between the resonant peaks. The absorption curve could be evened out using additional resistance in the neck, as shown in figure ???. Figure 21 shows the improvement in the absorption performance of the panel after adding neck perforations. Additional resistance improves the peak absorption value and the bandwidth of absorption. Hence, the resonant peaks merge into one another without deeper valleys.

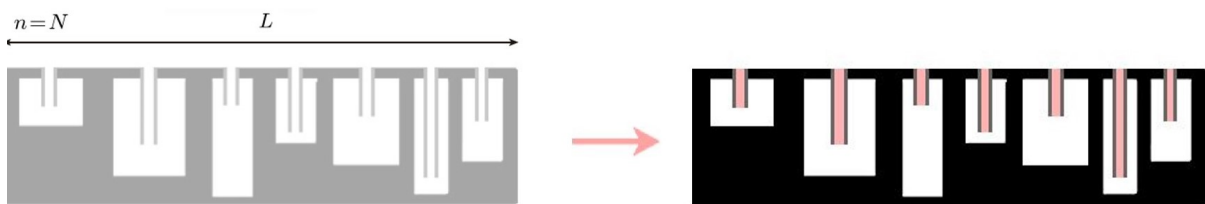


Figure 19: Enhancing the overall performance of the array through additional resistance in the necks of the resonators

Area = 619.2 < 64.7% >

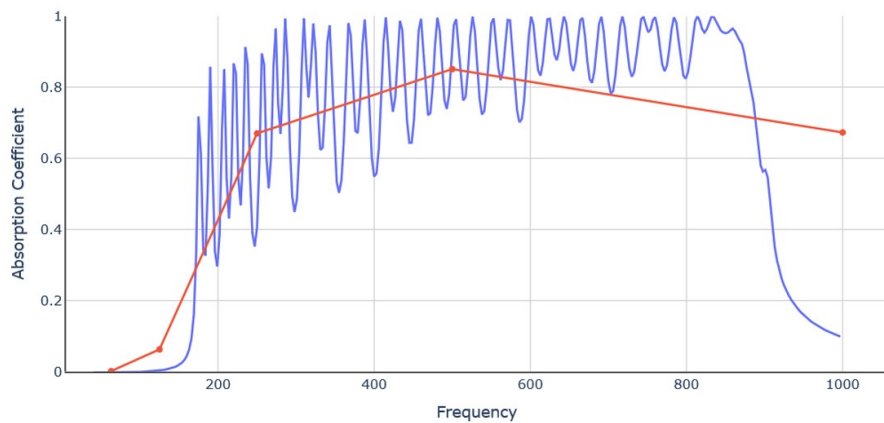


Figure 20: Results without additional neck resistance

Area = 727.2 < 76.0% >

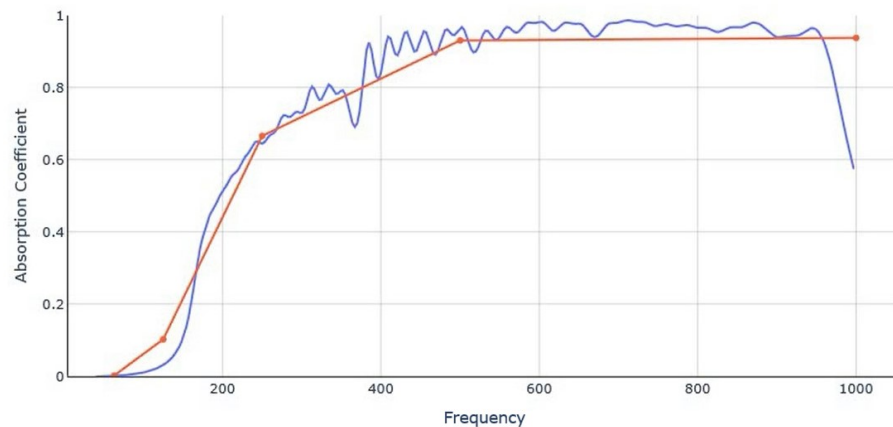


Figure 21: Results with additional neck resistance

4.4 Using the achieved absorption curve

The blue line in the graph of figure 21 shows the frequency-dependent absorption coefficients. This cannot be directly used in geometric acoustic simulation software; they require the values in octave bands. Octave filter is used for converting the frequency-dependent values to octaves-dependent that can be plugged into Pachyderm Acoustics for room simulation. This filter produces 8 discrete absorption coefficients, one for each octave band. The red line in the graph of figure 21 shows the octave filtered absorption values. These values are used to describe the absorption performance of a material in acoustics software.

4.5 The “best” panel

The advantage of the resonator panel design is that it can be customized to any frequency range. For example, to attenuate the excess noise in an engine room, a broadband absorber is not required but rather a targeted absorber. Figure 22 shows the absorption performance of a panel composed of low frequency resonators. With just 14 resonators, the absorption coefficient achieved is good in octaves 63Hz, 125Hz, and 250Hz. However, this panel is quite bulky—the panel size of about 0.3m x 0.35m and its depth is 0.16m. All the resonators have neck perforations and three have embedded necks to lower the resonant frequencies below 100Hz.

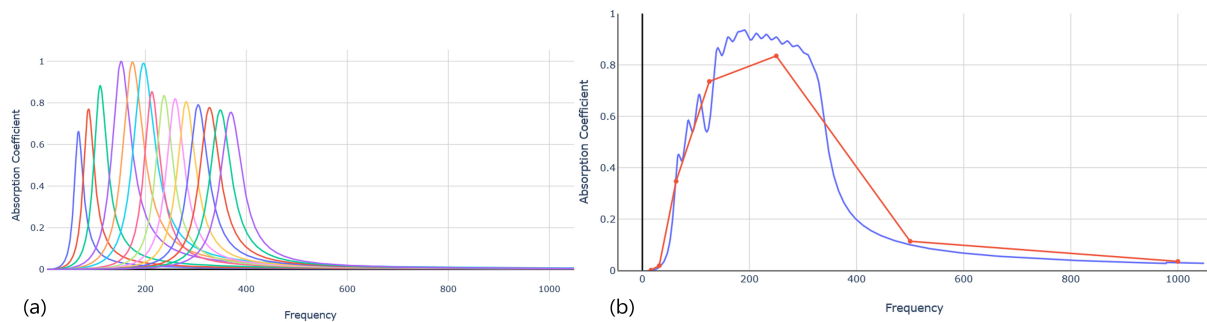


Figure 22: low frequency panel: (a) Absorption performance of the individual resonators in the panel; (b) Absorption performance of the panel

Another panel design for the mid frequencies is given in figure 23. This panel’s dimensions are similar to the low frequency panel, i.e., the area is 0.3m x 0.3m and the depth is 0.16m. However, due to the smaller size of the resonators required for attenuating mid frequencies, 36 resonators can be fit within this panel. This panel’s performance is improved with the use of neck perforations which produces good results in octaves 250Hz, 500Hz, and 1000Hz.

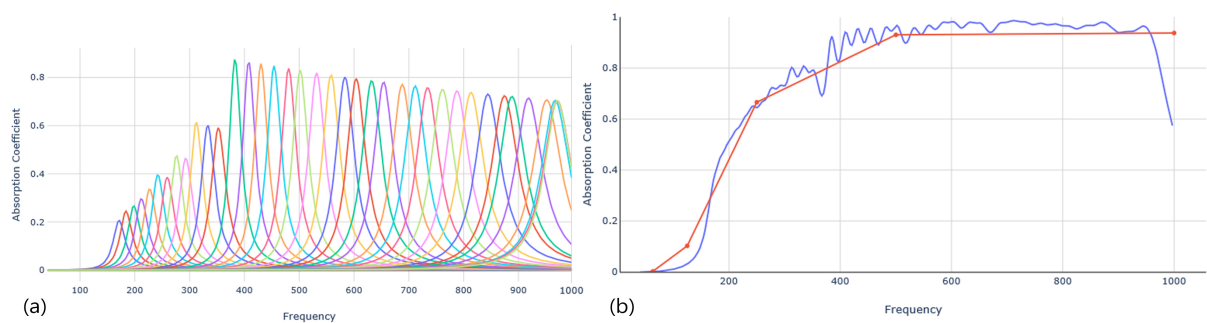


Figure 23: Mid frequency panel: (a) Absorption performance of the individual resonators in the panel; (b) Absorption performance of the panel

The absorption performances given do not factor in the material properties of the panel. In reality, this would further increase the absorption quality of the panel. Low-density MDF or plywood have adequate absorption in frequencies above 1000Hz and can positively impact the overall performance of the resonator panel. Thus, the choice of material can boost the absorption bandwidth of the panel.

5 Open office acoustics

Open office acoustics have been a source of discomfort for the employees. The acoustic conditions have an impact on the psychological and physiological well-being of the employees [Ebissou et al., 2015]. Most of the acoustic complaints are related to speech intelligibility and speech privacy in open offices [Delle Macchie et al., 2018]. The low partitions and the hard reflective wall surfaces bounce around the speech sounds causing a distraction to other employees. Two solutions are currently practiced in tackling this problem - sound absorption, and sound masking. Sound absorption is a passive technique and can be integrated within office furnishings. Sound masking is an active technique and requires loudspeakers to be installed in the ceiling. Both the techniques are usually implemented to improve the open office acoustics [Keränen et al., 2008, Bradley, 2004].

This research focuses on utilizing passive techniques in improving the open office acoustics. Instead of absorbing all the sound energy in the space and overlaying it with a masking sound, the prevalent background noise could help in masking the adverse effects of the irrelevant speech in open offices. The impact of a source speaker could be reduced by hindering the direct sound propagation and by minimizing its intensity through absorption. Frequency-specific sound absorbers, especially targeting the speech frequencies, can greatly lower the intensity of conversational sounds. This softer speech signal overlaid by the background noise from ventilation or hardware systems would be less detrimental to the work performance of other employees [Schlittmeier and Liebl, 2015].

The “best” panel described in the previous section was designed specifically for attenuating frequencies important for speech intelligibility. Introducing too much absorption in the space can make it very quiet and even a small disturbance can cause a distraction to a large number of workers. Hence, it is important to optimize the number of absorptive surfaces and their locations to maximize the acoustic quality. The knowledge of the optimal location could be derived from studying the nature of sound propagation in open offices. Placing the absorbers close to the source has proven to be fruitful [Fuchs, 2013].

5.1 Single-number acoustic parameters for open offices

Parameters to measure the loudness of the sound (SPL) or the speech intelligibility (STI) are spatial, i.e. they are dependent on the location of the speaker and the receiver in a space. Hence, they cannot be used to evaluate the acoustics of open offices where the speaker(s) and receiver(s) could be anywhere in the room [Schlittmeier and Liebl, 2015]. ISO standards for open offices [ISO 3382-3, 2012] gives four single-number parameters to measure the acoustic quality of an open-plan office. Distraction distance (r_D) is the radius from the speaker up to which people in that zone are easily distracted by the speech sounds. It is derived from the

spatial decay of STI values; r_D is the distance at which the STI value falls below 0.5. The spatial decay rate of A-weighted SPL of speech ($D_{2,S}$) is the rate at which the intensity of speech decreases when the distance is doubled. It is extrapolated from A-weighted SPL values measured at different locations in the open-plan. The third parameter is A-weighted SPL of speech at 4m from the source ($L_{p,A,S,4m}$). It is a straightforward measurement but is not necessarily measured first-hand. It can be obtained from a linear regression of A-weighted SPL values measured at various positions. The last parameter is the average A-weighted background noise level ($L_{p,A,B}$). Though this parameter is time-dependent, an averaged quantity helps estimate the masking of the intruding speech sounds.

Of all the four, r_D has the most direct correlation with the intrusion caused by speech sounds in open offices [Haapakangas et al., 2017]. It's based on STI which factors in the masking effect of background noise through signal-to-noise ratio estimation. While, $D_{2,S}$ and $L_{p,A,S,4m}$ depend on physical room parameters, such as the amount of absorption included in the room, the ceiling height, the shape of the room, its volume, and the inclusion of partition screens [Haapakangas et al., 2017], they are not affected by the background noise level which plays a major role in the speech intelligibility [Keränen et al., 2008]. Though r_D seems to be a promising indicator of the office acoustics, it cannot be solely dependent on for measuring the acoustic quality of the space without considering $D_{2,S}$, $L_{p,A,S,4m}$, and $L_{p,A,B}$. Small r_D values (which are favorable) can be obtained with high levels of background noise. But the acoustic comfort is poor with such high background noise. Hence, it is essential to consider all the four parameters while evaluating the acoustics of an open office.

The single-number parameters are simulated for one source speaker while the rest are silent receivers. This situation is considered to be the toughest to achieve good acoustics for. If multiple people are talking at the same time, their combined sound would create a better masking effect over the individual signals and the distraction caused is minor [ISO 3382-3, 2012]. The ISO also specifies target values for these parameters to achieve good open office acoustics.

Table 1: Target values of single-number parameters set by ISO

Parameter	Symbol	Target value
Distraction distance	r_D	$\leq 5m$
Spatial decay rate	$D_{2,S}$	$\geq 7dB$
SPL(A) at 4m	$L_{p,A,S,4m}$	$\leq 48dB(A)$
Background noise level	$L_{p,A,B}$	35dB - 45dB
Reverberation time	RT'60	0.7s - 0.8s

5.2 Room acoustic simulation

To study the open office acoustics, the geometry of the space is modeled in Rhinoceros 3D software. Real objects, like workstations and storage, are represented by 2D Surfaces in the Rhino interface. Complex geometry is abstracted to have a manageable simulation time. Pachyderm Acoustics, a plugin for Rhino software, is used for running the acoustic simulation. It provides additional properties to the 2D Rhino surfaces - absorption, scattering, and transparency coefficients in octave bands - to reproduce the real room characteristics. A variety of acoustical analysis can be run with a source and multiple receivers.

5.2.1 Office layouts

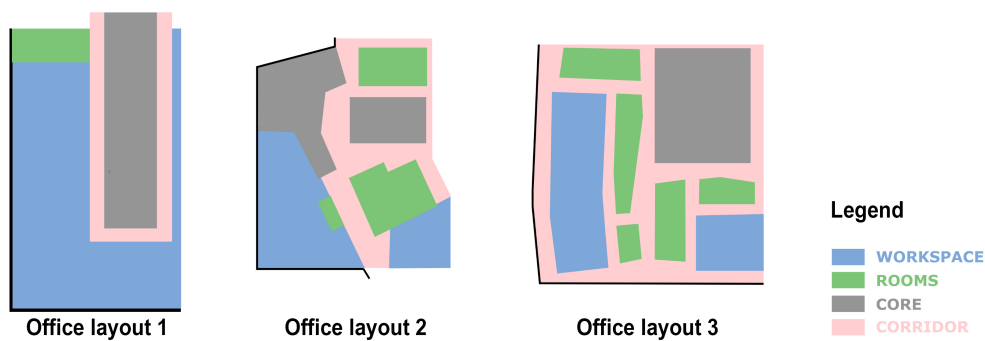


Figure 24: Different open office layouts for simulation

Three variants of open offices are studied to estimate the effectiveness of the Helmholtz resonator panel. Figure 24 shows the layouts of the three case studies which are modeled based on existing open offices in the US (made anonymous). It might be computationally expensive to simulate the acoustics for the whole floor plate. Hence, a representative section of the floor plate is used for the room acoustic simulations. The three layouts chosen have different levels of visual privacy and isolation from common areas. Hence, each type has a different level of background noise in the workspace area, the total area of vertical absorptive surfaces, and the workstation setup. Acoustic simulation of these layouts in its existing conditions and a scenario with resonator panels are performed for assessing the acoustic improvements possible with resonator panels. A full report is given in the case studies section.

5.3 Study methodology

To study the impact of the Helmholtz resonator panel (HR panel) on the open office acoustics, a simple office layout (figure 25) was modeled. It is a rectangular layout of 16m x 33.5m with a ceiling height of 3.2m and has a single main corridor that connects the workstations to the central circulation zone. Each workstation is L-shaped (dimensions 2.6m x 2.4m) and groups of eight workstations make a bay. The bays are arranged parallel to each other with a walking gap of 1.4m.

The measurement of the acoustical quality is carried out as per the ISO standards. Two lines of measurement that overlap with the seating positions, as specified in figure 25 (b), are used for simulating the acoustic condition of this layout. At the intersection of the two lines is the position of the sound source and all the other dots are receivers. The source, a geodesic omnidirectional source, is defined with a speech power level in octave bands for normal effort speech as specified in ISO 3382-3 [ISO 3382-3, 2012]. The receiver positions have microphones for recording the impact of the source speaker at that respective location. The source and the microphones are placed at 1.2m from the floor level to mimic seated workers. A background noise level is applied to imitate real office conditions.

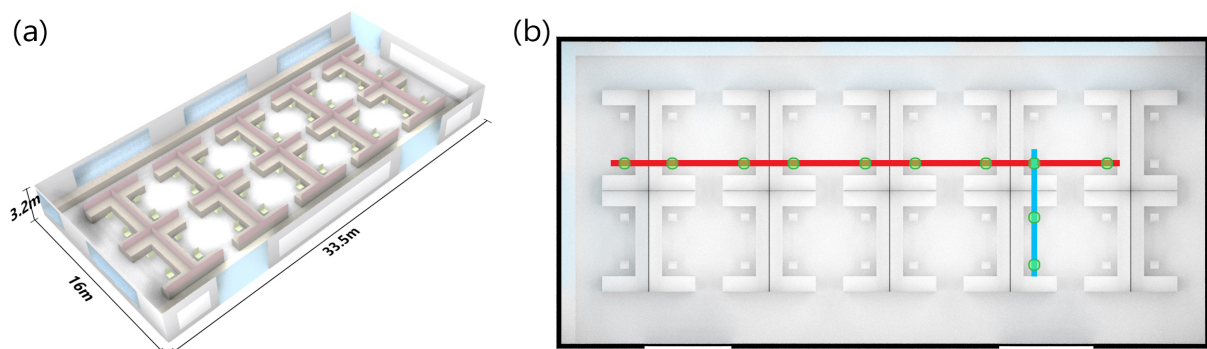


Figure 25: (a) View of the simple layout; (b) Plan overlaid with the two lines of measurement

5.3.1 Background noise levels

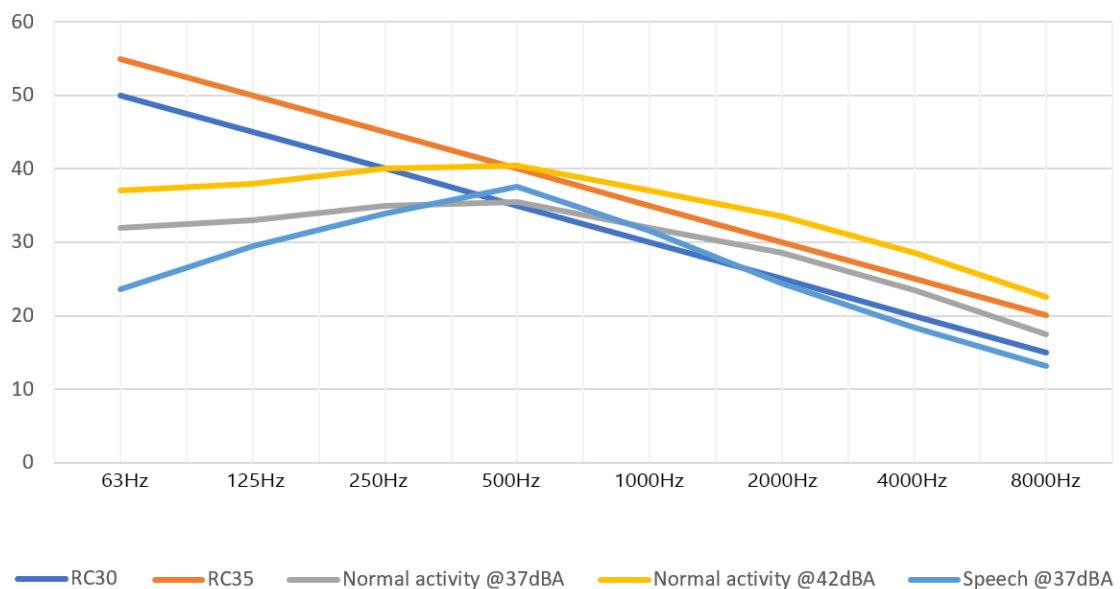


Figure 26: Background noise levels used in the open office simulations

Speech intelligibility in open offices is measured using STI which factors in the useful signal to the background noise ratio. To achieve good acoustics that does not interfere with the employee's work productivity, the STI value has to be maintained within 0.2 (refer figure 4).

Higher levels of background noise can achieve this value but ISO sets the acceptable range to be within 35dBA - 45dBA. Hence, background noise levels of 37dBA and 42dBA were used for acoustic studies.

Room Criteria (RC) noise curves provide a range of allowable background noise levels in a room. It is specifically used for modeling the HVAC systems in a space. RC30 and RC35 curves, corresponding to 37dBA and 42dBA, are used for reproducing background noise from air vents in the open office simulation. Background noise levels measured in the presence of normal human activity, given in [Nilsson and Hellström, 2010], were also used in the studies. Finally, the speech signal was used as background noise to simulate multiple speakers in the office.

5.3.2 Panel distribution in the open office

To study the influence of the number of absorptive surfaces in achieving good acoustics, a series of instances with an increasing number of ceiling-hung HR panels were introduced. The combined area of the panels in each instance is expressed as a percentage of the workstation area. The nine variations had a uniform arrangement of panels around each workstation maximizing the mitigation of the reflected sound waves between workstations. (see figure 27).



Figure 27: Arrangement of ceiling-hung panels in each instance

5.3.3 Panel heights

To optimally locate the panels in the open office, the heights of the ceiling-hung panels were varied from 2.1m to 3.1m in increments of 0.2m while keeping the ceiling height fixed. The

height of the panels impacts the amount of direct sound energy reaching the panels (based on solid angles) and the early reflection time of the speech sound. When the panels are closer to the source speaker, a large portion of the speech energy reaches the panels when compared to the case where the panels are farthest from the speaker. Low-hung panels also reduce the travel distance of the reflected sound waves, and hence reduces the early reflection time at the receiver’s location. This reduces the reverberation time as well, since early reflections are the largest contributors to the RT60 measurement.

5.3.4 Multi-objective problem

There is a direct correlation between the amount of absorption and the overall sound energy in the room. Covering the whole ceiling area with absorptive panels can result in a quiet environment (refer figure 28). However, this does not necessarily create an acoustically comfortable environment. Employees prefer to work in the presence of ambient noise, which is not too loud since it helps mask the intruding speech signals. This essence is captured by the distraction distance parameter. Hence, r_D does not exhibit a linear relationship with the number of absorptive surfaces introduced. With an increasing area of absorptive surfaces, the excess sound energy in the space decreases which lowers the r_D . The r_D dips when it reaches the balanced ambient noise level. This is the optimal amount of absorption as further increasing the area of absorption will start to increase the r_D . Figure 28 shows the dynamic relationship between the distraction distance and the amount of absorption. The green zone marked points at the optimal amount of absorption in the space for which r_D is the least.

To strike the right balance in achieving good acoustics, the number of absorptive panels introduced in the space will have to be modulated with r_D and $D_{2,S}$. The spatial decay, $D_{2,S}$, controls how much of the originating sound energy gets dissipated with distance doubling. Large $D_{2,S}$ value results in smaller overall sound energy in the room. $D_{2,S}$ cannot be maximized without degrading the r_D and vice versa. Hence, multi-objective optimization was utilized for the balancing act of finding the optimal amount of absorption, which maximizes the $D_{2,S}$ but also minimizes the r_D .

The multi-objective algorithm used for this parametric analysis is Pareto sorting. It produces a set of optimal solutions, called the Pareto frontier, for two or more fitness functions in which each solution does a good job on all the fitness functions given and is not the best-case for the fitness functions individually.

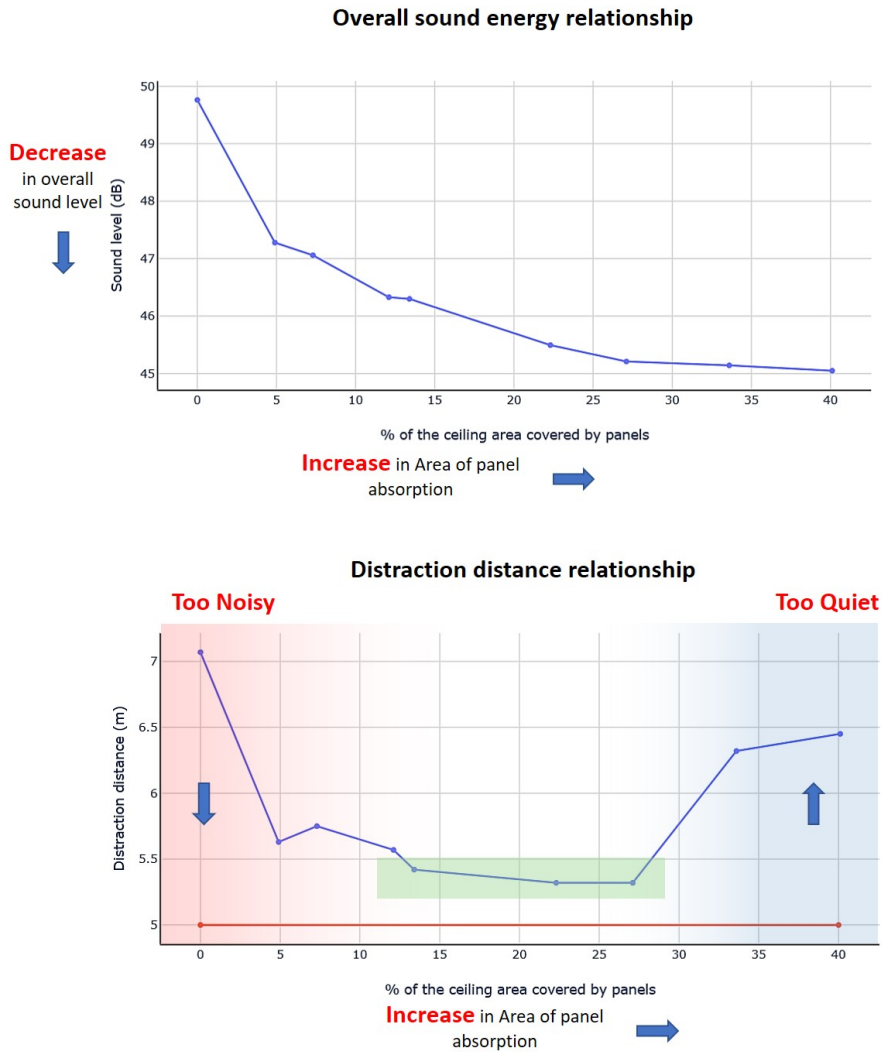


Figure 28: (Top) Linear relationship between the overall sound energy and the amount of absorption; (Bottom) Dynamic relationship between the distraction distance and the amount of absorption

5.4 Study 1 - Efficiency of the resonator panel

The simple office layout, as described in section 5.3, was furnished with 1.5m high desk partitions made of foamy infill with fabric encasing. An acoustic simulation set was run for different ceiling-hung HR panel distributions (section 5.3.2) located at varying heights (section 5.3.3) from the floor level. Speech intelligibility (STI) was calculated using the background noise levels discussed in section 5.3.1. To gauge the efficiency of the resonator panels, the same simulation set was repeated with traditional porous ceiling tiles instead of the resonator panels (see figure 29). Of the various combinations between the panel distributions and their heights from the floor level, the same scenario is selected from both the simulation sets to study which absorber performs well in improving the open office acoustics. The spatial acoustic quality in both cases is given in figure 30.

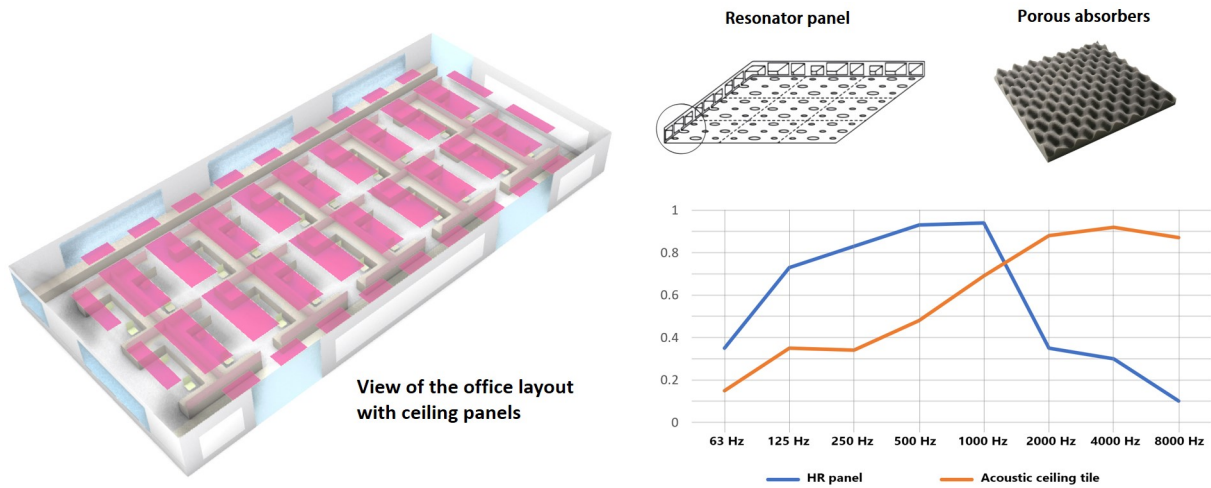


Figure 29: (Left) Open office setup for comparing the efficiency of the resonator panels and the porous acoustic tiles; (Right) Absorption performance of the resonator panel and the porous ceiling tile

The sound energy distribution in both the cases (measured in dBA) is mapped out in figure 30. The lower end of the scale is limited to 30 dBA since values lower than that are not considered disturbing. Considering stark differences cannot be noticed with the heatmap colorscale, a delta map is plotted from the difference in their energies. In the delta map, the white color depicts the zero difference zone while green depicts the highest difference. The largest green zones are observed in the workstation bays right next to the speaker, with a difference of almost 5dBA. This shows that the HR panels are efficient at limiting the sound propagation when compared to acoustic tiles.

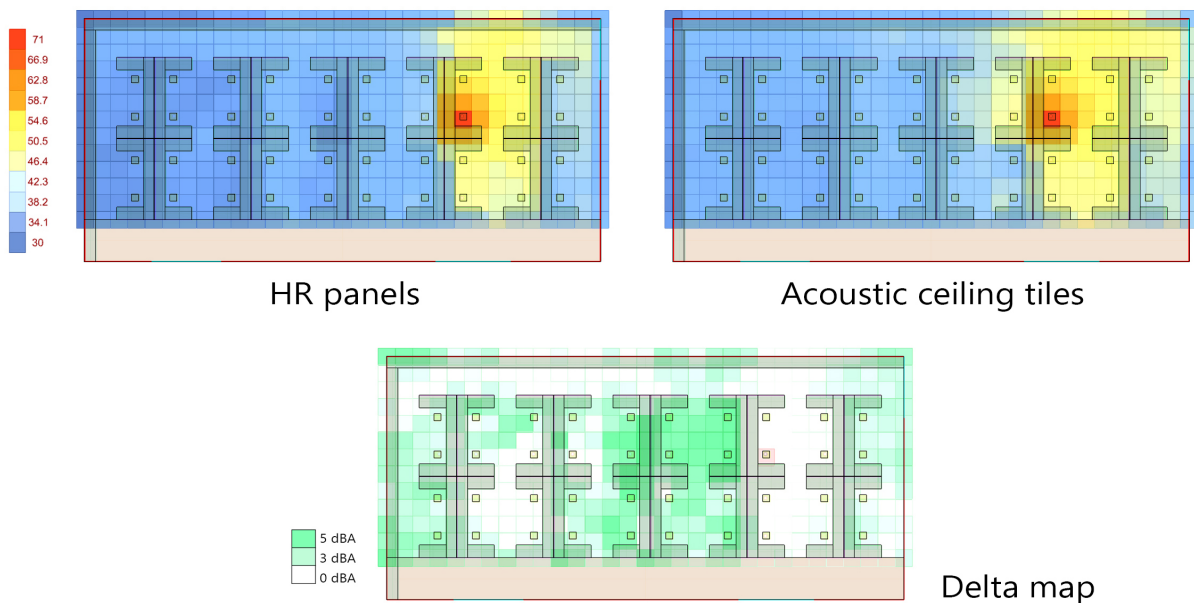


Figure 30: Sound energy distribution in the open office under the two panel scenarios and their delta map

5.5 Study 2 - Benchmarking with conventional offices

The CBE survey results show that cubicle-styled traditional office layout with high partitions acoustically performs better than an open office with low partitions. Therefore, a conventional workspace style was modeled in the same simple layout by enclosing the workstations on three sides by 1.7m tall partition walls made of foamy infill with fabric encasing. The results from this study served as a benchmark for achieving good acoustics in open offices with low partition walls.

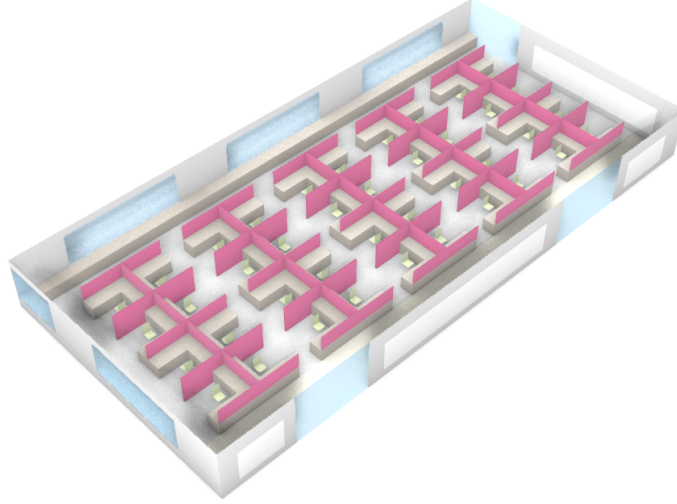


Figure 31: Model of a cubicle-styled traditional office layout

The same combination technique was used in this study - scenarios of different panel distributions at varying heights are incorporated in the cubicle-style layout for acoustic simulation. A full report of this study is given in appendix I. To obtain the best performing scenarios, Pareto front analysis was performed. The fitness criteria utilized are to minimize the area of absorptive panels (indirectly, the cost), to minimize the r_D (ISO's target is $r_D \leq 5$), and to maximize the $D_{2,S}$ (ISO's target is $D_{2,S} \geq 7$). These three fitness functions are plotted on the three axes of a 3D graph and each 2D section of the 3D graph is given in figure 32. The green region marked in these sections correspond to the ISO's target values for the single-number parameters essential for achieving good acoustics (refer table 1). A gradient is applied for the area of absorption axis because it is a subjective choice to minimize the cost invested in the HR panels. The red dots in these sections point out the Pareto frontier scenarios and this set is considered favorable to all the fitness functions used. Within this set, a few of the scenarios which lie within or in the vicinity of the green region are selected as candidate scenarios.

Apart from distraction distance and spatial decay rate, ISO suggests other single-number parameters to measure the acoustic quality of an open office. For the candidate scenarios, a spider chart with axes representing the single-number parameters recommended by ISO is depicted in figure 33. The different value ranges of these parameters are modulated to a 1 - 5 spider plot scale. This conversion is given in Appendix C. The green region in the center of the

chart delineates the values that fall within the ISO's benchmark. The aim is to get the blue lie to fall within the green zone.

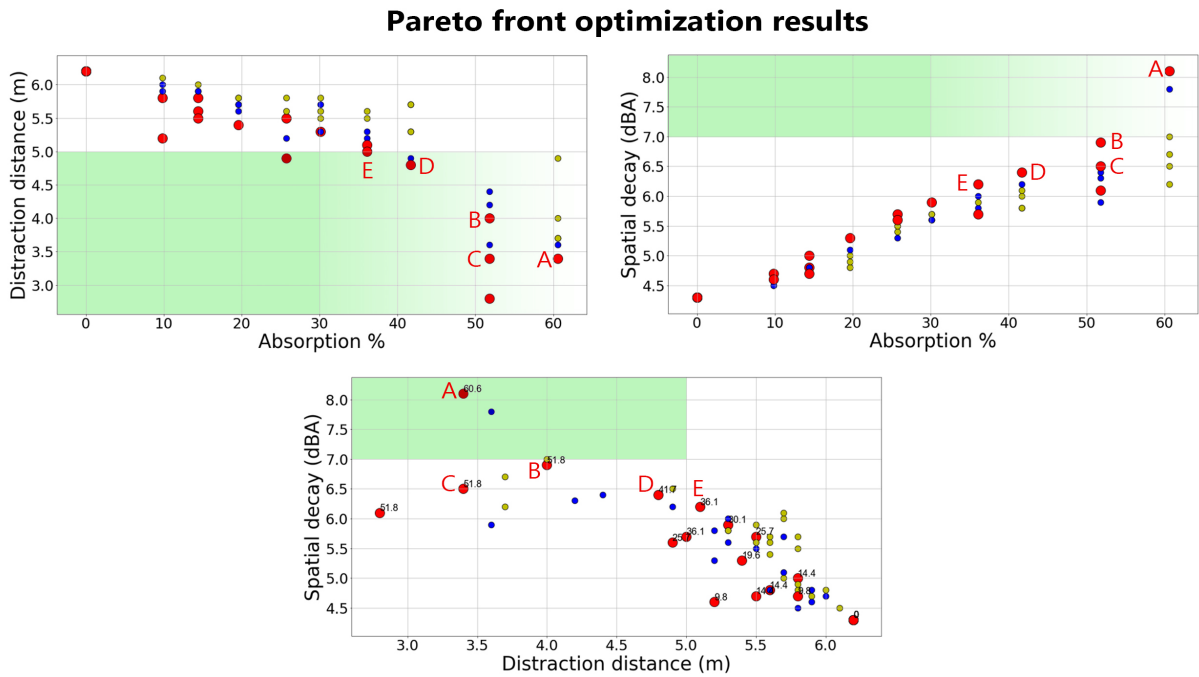


Figure 32: Pareto front sections

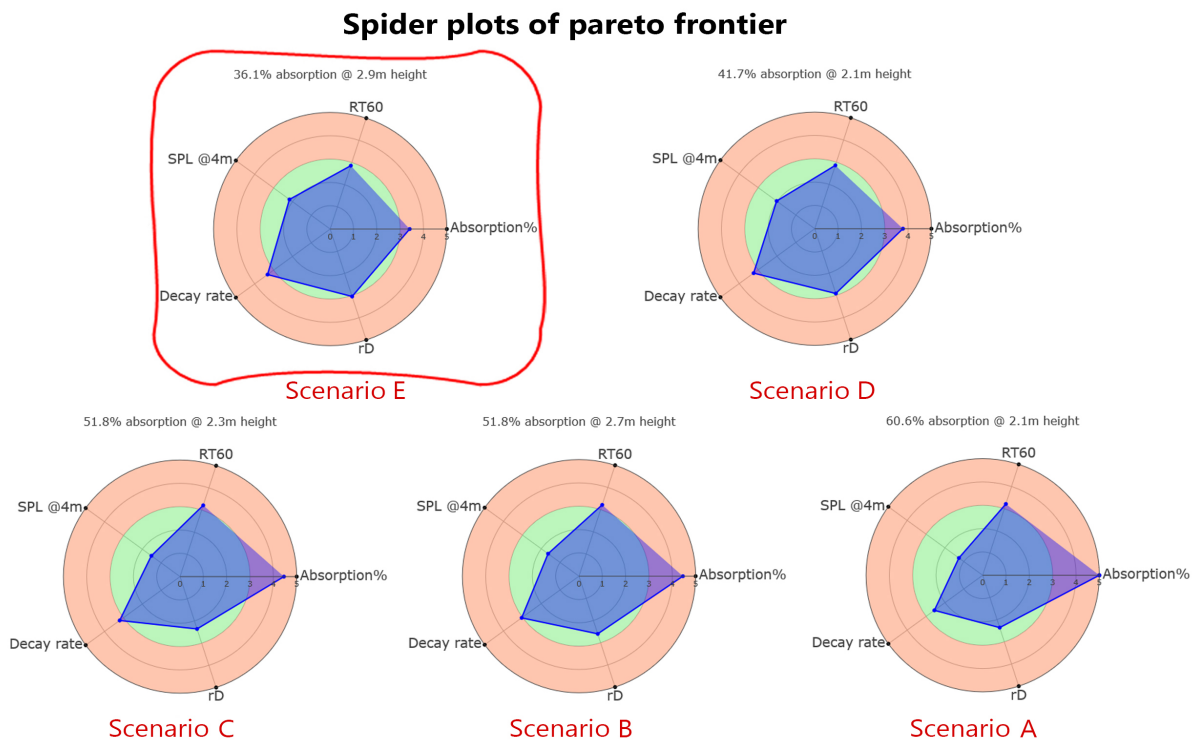


Figure 33: Spider plot analysis of the candidate scenarios in the Pareto frontier

From the spider plots (figure 33), it is clear that no scenario falls completely within the green zone. Improving one or some of the parameters curtails the others. Hence, some trade-offs must be made in choosing one scenario over the other candidate scenarios. The scenario E which has 36.1% area of the ceiling covered by the HR panels at the height of 2.1m from the floor level is an interesting solution. Though the spatial decay is just outside of the target values set by ISO, the other single number parameters have satisfactory results. Increasing the area of absorptive surfaces improves the spatial decay but reduces the reverberation time in the open office well below the comfortable range. This is the case with scenario A which has 60.6% area of the ceiling covered by the HR panels. Such a high percentage might not be a feasible solution in terms of the cost invested in the panels. The same trends are observed in scenario B (51.8% HR panel absorbers @ 2.7m height) and scenario C (51.8% HR panel absorbers @ 2.3m height); a large area of absorption negatively impacts the reverberation time and increases the expenses. Between these two scenarios, there is a marginal difference in their decay rates caused by the location of the HR panels. Scenario D, which has 41.7% panel area coverage, has satisfactory single-number ratings and has a similar acoustic response to that of scenario E (36.1%) expect in the spatial decay parameter. This small difference could be seen as a trade-off with the cost of investment. Therefore, scenario E is a cost-effective solution that can achieve good acoustics.

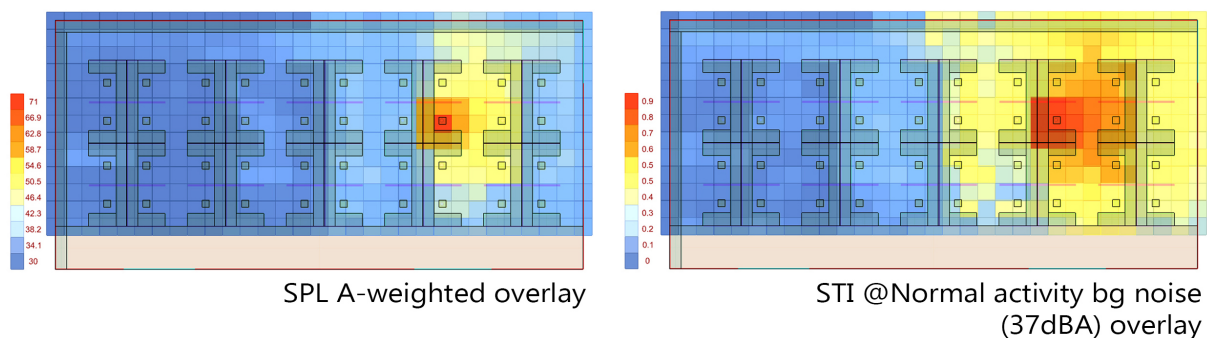


Figure 34: Scenario E - Spatial sound distribution maps of the conventional layout

5.6 Study 3 - Flat vs. Tilted HR panels

This study tests the efficiency of the ceiling-hung HR panels for two different orientations. The first case, flat ceiling-hung panels, has all the panels facing down towards the workstations. In the other case, the panels are angled to face the speakers or the chair locations. The tilted ceiling-hung panels are designed by pitching the flat panels along the centerline. They form a “V” and are anchored right above the partitions and bays that separate two workstation rows. These panels were modeled in the same layout as described in section 5.3. A set of simulations were run for each type of panel orientations.

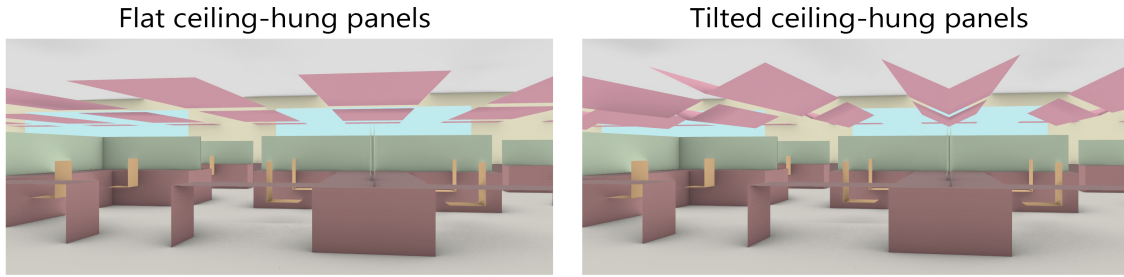


Figure 35: Views of the open office with flat and tilted ceiling-hung HR panels

The same scenario - 30.1% area of the ceiling at 2.3m height from the floor level - is picked up from both the simulation sets for comparison. To portray the efficiency of tilted panels over flat panels, sound energy distribution in the open office with flat and tilted HR panels is given for comparison (see figure 36). It is clear that the tilted panels do a better job of containing the sound. The delta map shows the difference in the sound energies and the green zone depicts the highest energy difference zone. The large green zone two workstations away from the speaker show the tilted panel's efficiency in restricting the speech signals from affecting a lot more people. This is because the tilted panel reflects the sound back to the speaker instead of spreading it. The difference observed is almost 6.5dBA which makes a significant difference in the acoustic quality in that zone.

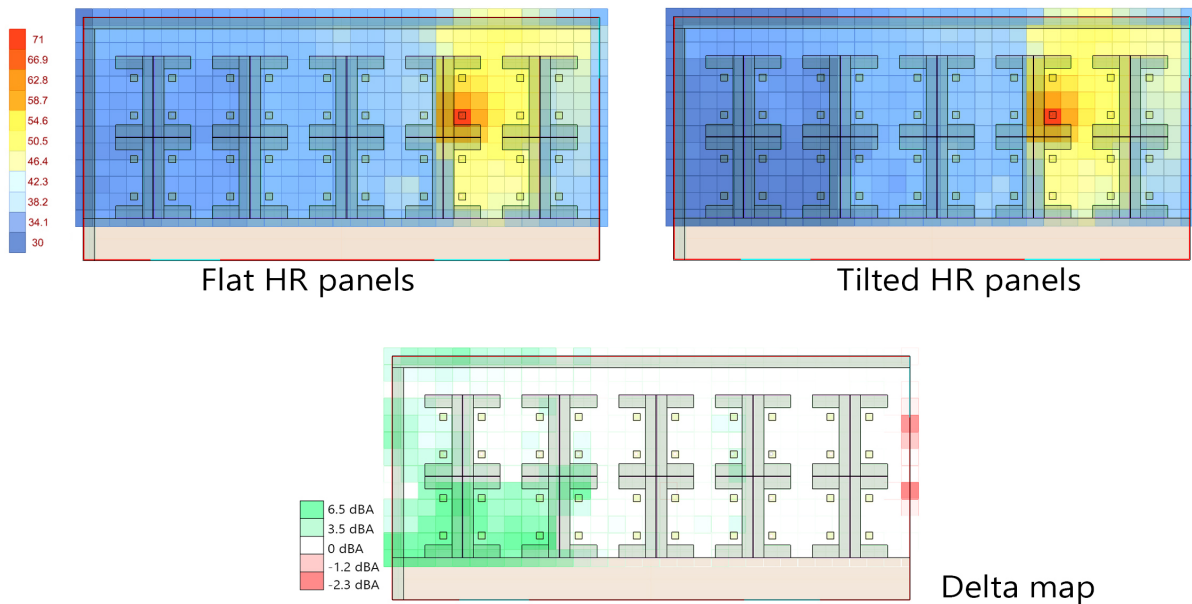


Figure 36: Comparative analysis between flat HR panels covering 30.1% area of the ceiling at 2.3m height from the floor level vs. Tilted HR panels covering 30.1% area at 2.3m height

6 Open office case studies

The three office layouts discussed in section 5.2.1 are tested for their acoustic performance and improvements using HR panels are suggested for each layout. These case studies are existing offices in the US and a representative section of the floor-plate is used in the simulations. The baseline scenario encompasses the existing conditions in the office space, including the materials used. The improvements to the office space are executed with two strategies - changing the desk partition material to fabric encased foam infill material, and replacing the acoustic ceiling tiles (ACT) with tilted HR panels.

6.1 Office layout 1

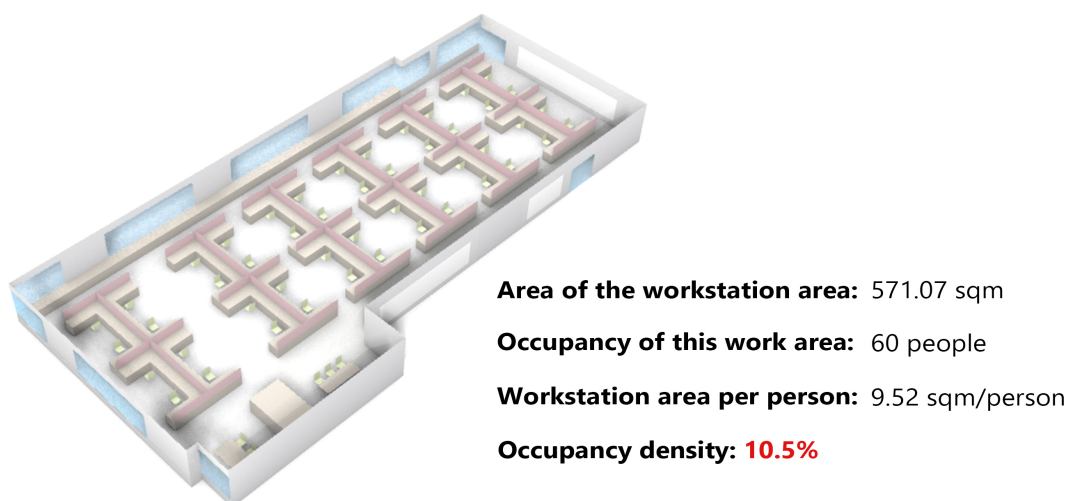


Figure 37: View of office layout 1 and its occupancy density

Layout 1 has a single main corridor that runs around the core of the building and connects the workstations to the main lobby and kitchen area. Meeting and conference rooms, on one end, isolate this workstation area from the public gathering spaces and provide visual privacy. On the other end, the collaboration area provides the disconnect from another similar workstation zone around the core. The work area is not densely populated and there is a sufficient buffer between the workstations. Mini enclosures are formed by the desk partitions promoting team spaces of 4 seats. This ensures worker collaboration and keeps in check the distraction caused to others.

6.1.1 Baseline scenario

Figure 38 shows the baseline scenario of office layout 1. The highlighted rectangles are acoustic ceiling tiles adhered to the ceiling over each workstation bay. The area of the tiles covers 64% of the workstation area. The desk partitions are made of metal panels and sit

0.6m from the table height. The spider chart is used as an acoustic rating system to compare the baseline scenario with the improvement scenarios. Each axis represents a single-number acoustic parameter – like distraction distance, reverberation time, spatial decay, and SPL at 4m from the speaker. ISO has set target values for these parameters in achieving good open office acoustics (refer table 1). The green zone marks the good acoustics zone. The baseline scenario achieves a good value on most of the parameters except the spatial decay parameter.

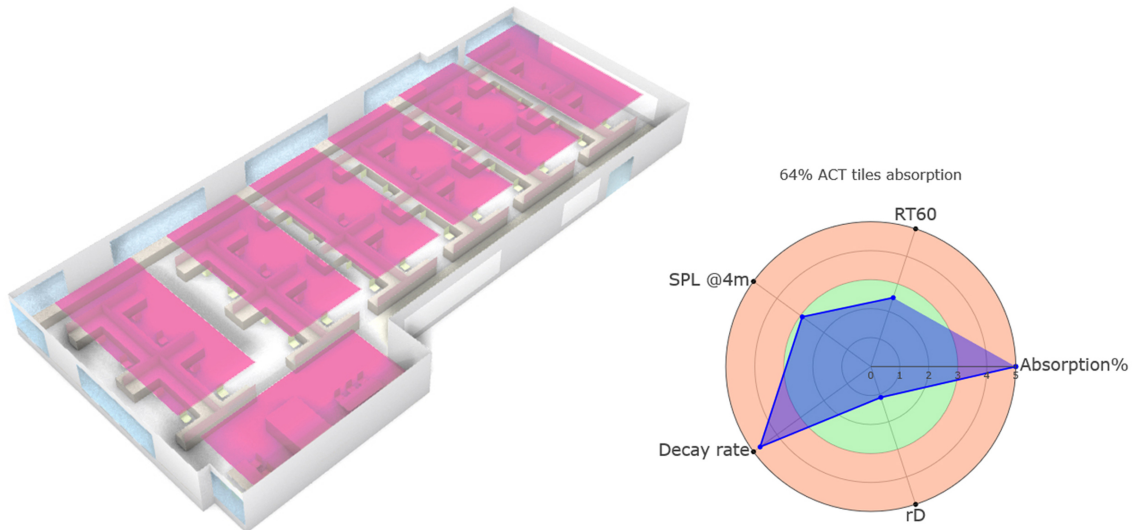


Figure 38: View of the baseline scenario with highlighted acoustic ceiling tiles and its spider plot rating

6.1.2 Improvements with HR panels

Two sets of improvements are performed on this layout. First, the desk partition height is increased to 1.5m (or 0.75m from the table height) and the material is switched to fabric encased foam infill. Second, the acoustic ceiling tiles are swapped with HR panels. To understand the optimum area of HR panels needed for this layout, 8 successively increasing areas of HR panel distributions are used in constructing the height vs. area of absorption matrices (as discussed in section 5.4). The area of the panel distributions and the matrices are given in Appendix J. Pareto front analysis is applied on all the scenarios in the height vs. HR panel area matrix, given in figure 39. All the scenarios except for the 0% absorption fall within the ISO’s target range for distraction distance, owing to the low occupancy density and the large volume of the space. However, due to the same reasons, the target value of spatial decay is not met. Such a large space would require a substantial quantity of absorbers to achieve the target value. Still, the spatial decay values achieved by the candidate scenarios A B are acceptable. The candidate scenarios are further explored through spider graph acoustic rating (refer figure 40).

Pareto front optimization results

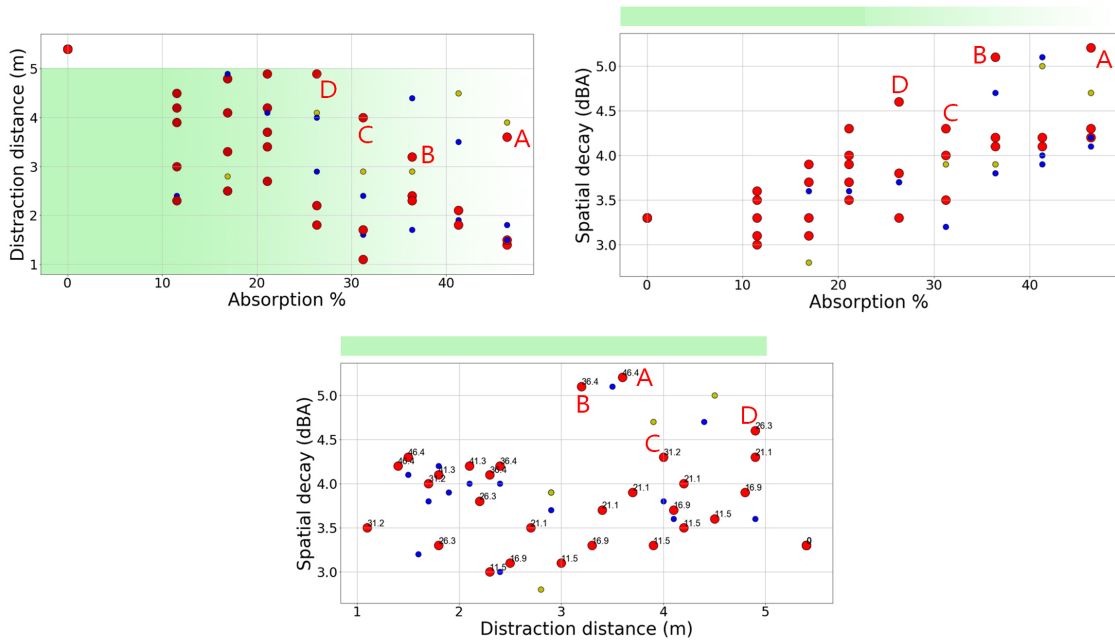


Figure 39: Pareto analysis of the different HR panel configurations

Spider plots of pareto frontier

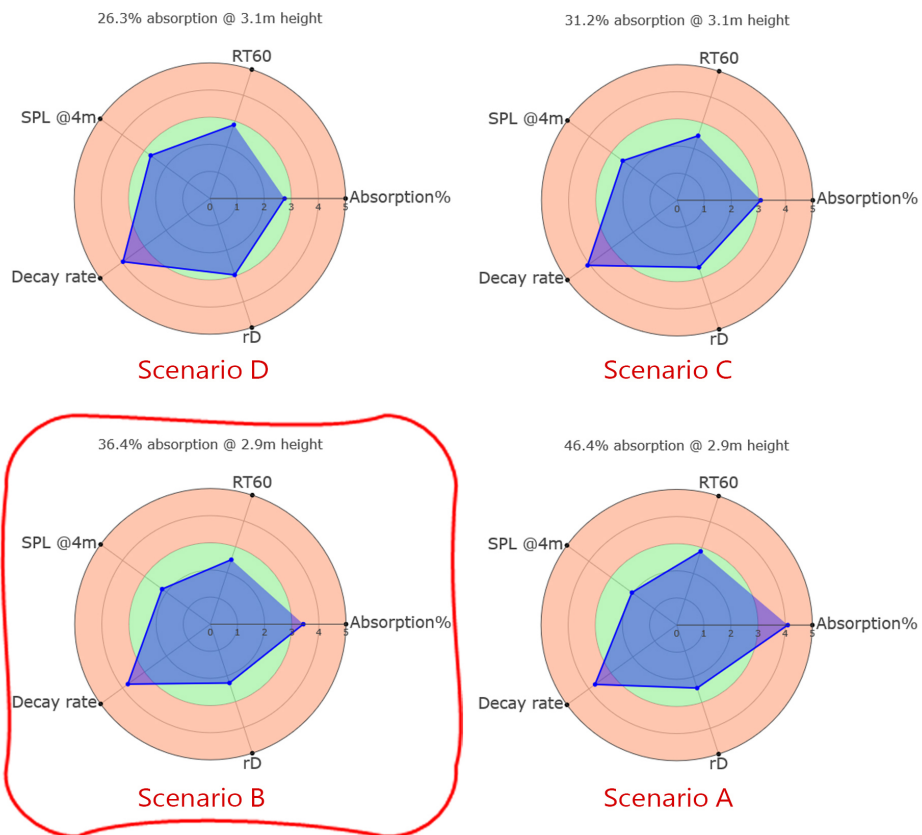


Figure 40: Spider plot analysis of the Pareto scenarios

Four different areas of absorption are in the candidate solution set - 26.3% (Scenario D), 31.2% (Scenario C), 36.4% (Scenario B), and 46.4% (Scenario A). All the scenarios have satisfactory values in each of the parameters except in spatial decay. The spatial decay improves with increasing area of absorption but both scenarios A (46.4%) and B (36.4%) exhibit similar spatial decay values. Scenario B is the most cost-effective scenario that can achieve good acoustics and hence is chosen as the best-case scenario. Figure 41 shows the layout's improved case with scenario B HR panel distribution.

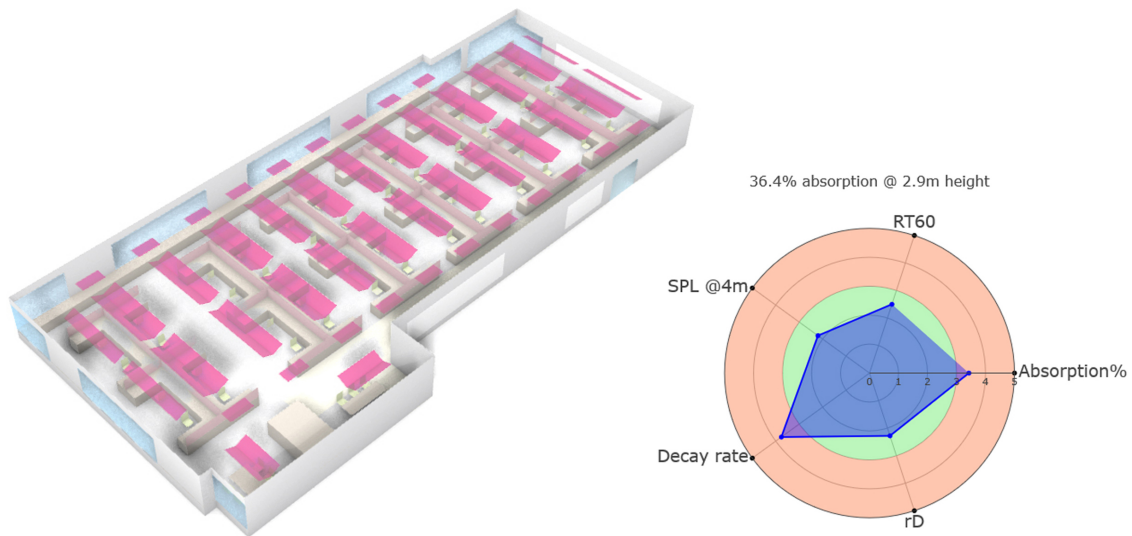


Figure 41: View of the best-case scenario with highlighted HR panel configuration and its spider plot rating

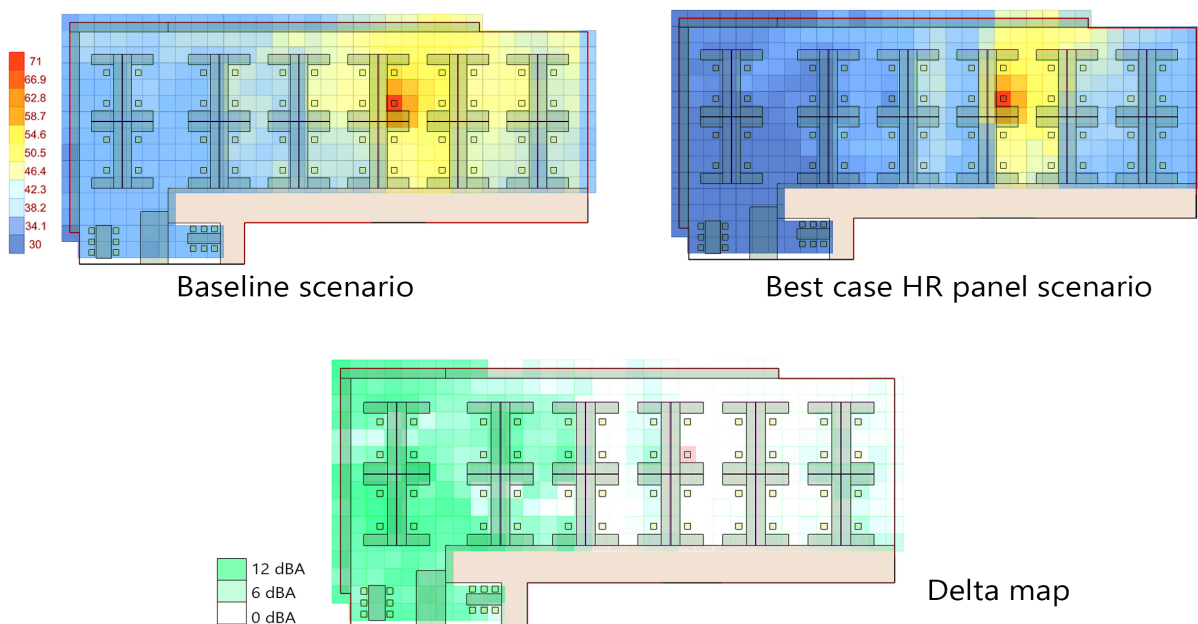


Figure 42: Sound energy distribution in the baseline scenario and the best-case HR panel scenario and their delta map

The sound pressure distribution in the layout from a single source speaker is compared between the two scenarios - the baseline case, and the improved case with HR panels. Even from the heatmaps, it is clear that the best-case scenario performs well in containing the speech sounds. A delta map is produced from the energy differences between the two scenarios. The white zone depicts zero energy difference while green depicts the highest energy difference. A 10dBA improvement is achieved one workstation away from the speaker and up to 12dBA improvement at three workstations away. This is a very noticeable improvement at the receiver locations. For the same best-case scenario, simulations are generated for multiple speakers (given in figure 43). For two simultaneous speakers, there is a good acoustic screening effect observed at most of the employee locations in-between the sound sources. When a third speaker is introduced in the corridor space, the acoustic quality deteriorates because of the insufficient amount of absorption over the corridor space.

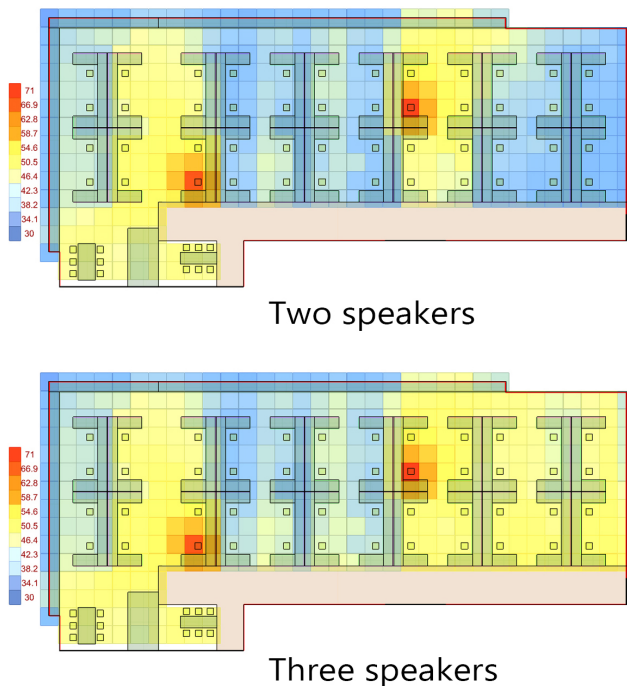
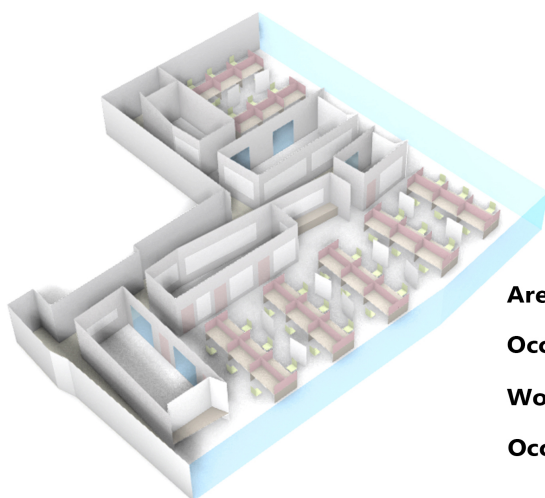


Figure 43: The best-case HR panel scenario with simultaneous speakers

6.2 Office layout 2



Area of the workstation area: 385.88 sqm
Occupancy of this work area: 42 people
Workstation area per person: 9.19 sqm/person
Occupancy density: **10.9%**

Figure 44: View of office layout 1 and its occupancy density

Layout 2 has two layers of circulation - the main public corridor that wraps around the core, and a semi-private corridor that wraps around the workstation area and connects it to the main corridor. Hence, a signification visual privacy and acoustic isolation from the public spaces. In between the two corridors, focus rooms and collaboration spaces are nestled creating an acoustic buffer. The workstation area is split into smaller areas of 30-seater workspaces connected through a breakout area. The walls of the breakout area are lined with acoustic felt to contain the sound propagation between work areas. Within a work area, rows of workstations are separated by movable whiteboards to create some acoustic privacy. The proximity of workstations in this layout is much closer than layout 1, and hence the occupancy density is slightly lower than layout 1.

6.2.1 Baseline scenario

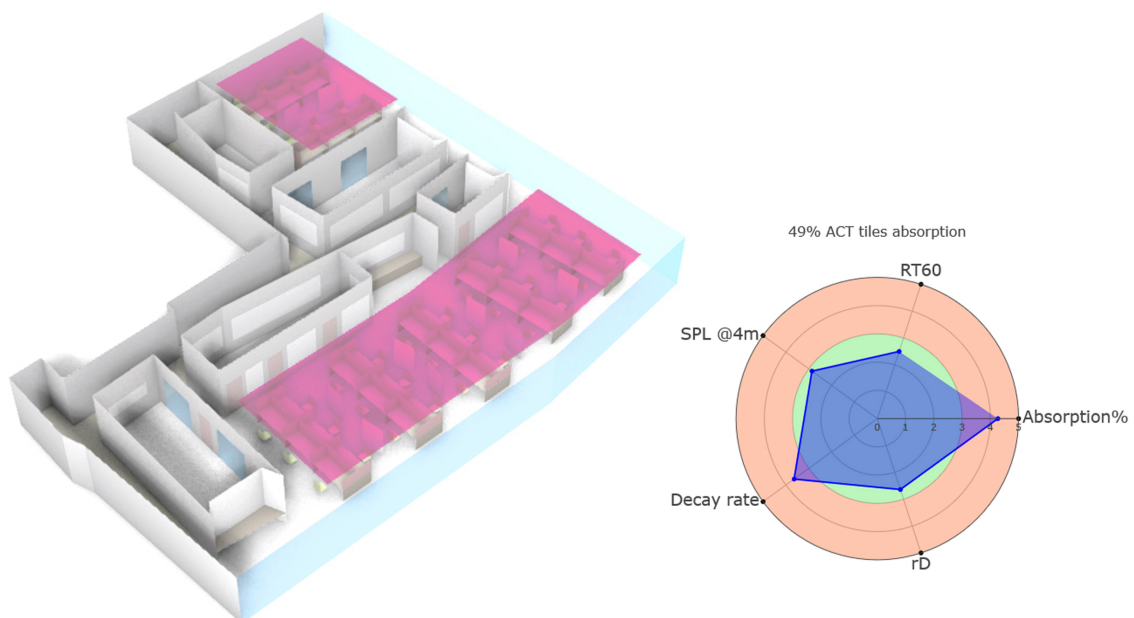


Figure 45: View of the baseline scenario with highlighted acoustic ceiling tiles and its spider plot rating

The baseline scenario of layout 2 is given in figure 45. The desk partitions are made of acoustic material with 0.45m of glass at the top. The highlighted rectangles are acoustic ceiling tiles at 2.3m from the floor level concealing the ductwork and electrical wiring above. 49% of the workstation area is covered by the acoustic ceiling tiles. A band of painted gypsum ceiling runs along the perimeter in plane with the rectangular tiled area. This low-height false ceiling over the workstation zone works well in maintaining the acoustic parameters within the ISO's target range except for the spatial decay parameter, as depicted in the spider chart.

6.2.2 Improvements with HR panels

Again, two sets of improvements are performed on this layout. The height of the desk partition is maintained the same but the material of the whole partition is switched to fabric encased foam infill. A successively increasing area of HR panel distributions is designed to study the optimum area of tilted HR panel absorbers. The same height vs. area of absorption matrix is used for studying the trends and applying each scenario into Pareto front ranking. The area of the panel distributions and the matrices are given in Appendix J. In the Pareto front results (see figure 46), approximately one-fourth of the scenarios fall within the ISO's target range for distraction distance. This portion is lesser than the one observed in layout 1 and can be attributed to the reduced occupancy density in layout 2. For the same reason, the spatial decay values of the candidate scenarios are marginally higher than the values attained in the improved layout 1. Though these values do not fall within the ISO's target range, they are acceptable. The candidate scenarios are further explored through the spider plot acoustic rating (figure 47).

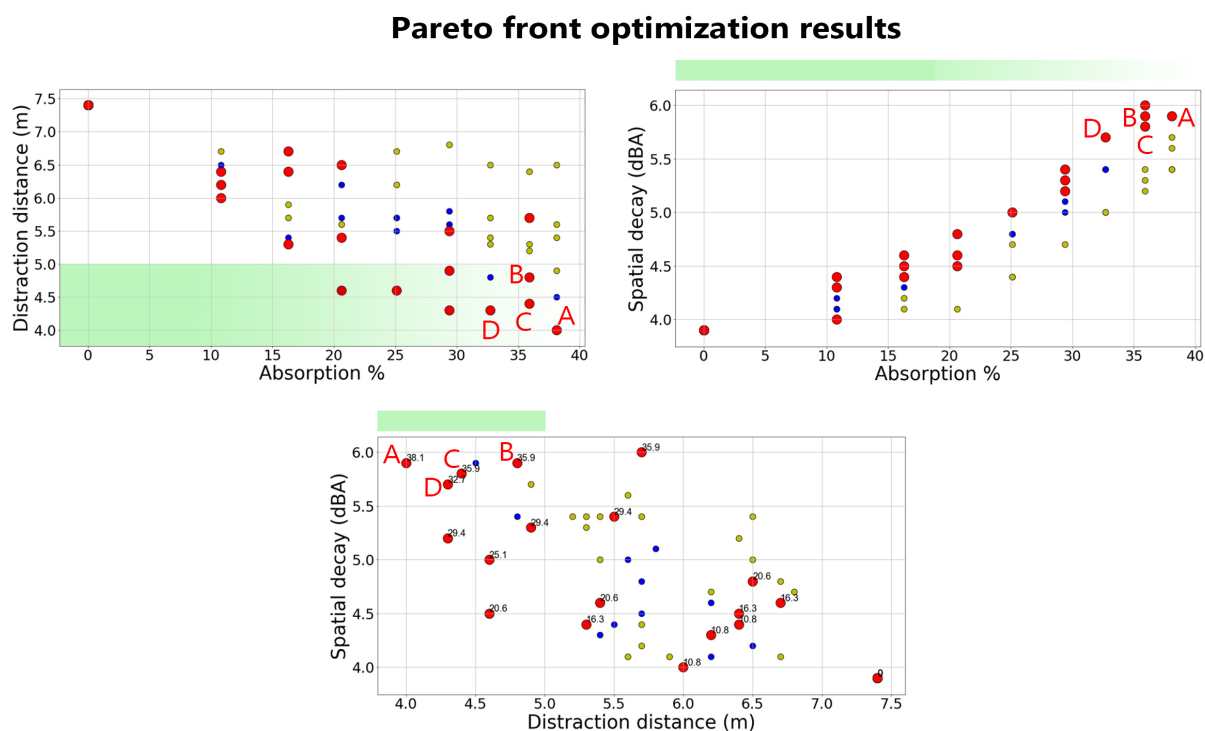


Figure 46: Pareto analysis of the different HR panel configurations

Three different areas of absorption are in the candidate solution set - 32.7% (Scenario D), 35.9% @2.1m height from the floor (Scenario C), 35.9% @2.3m height from the floor (Scenario B), and 38.1% (Scenario A). All the scenarios have satisfactory values in each of the parameters except in spatial decay. The spatial decay improves with increasing area of absorption but both scenarios A (38.1%) and B (35.9%) exhibit similar spatial decay values. Scenario B is the best-case scenario because the HR panels are hung at 2.3m from the floor which emulates

the baseline scenario. Figure 48 shows the layout's improved case with scenario B HR panel distribution.

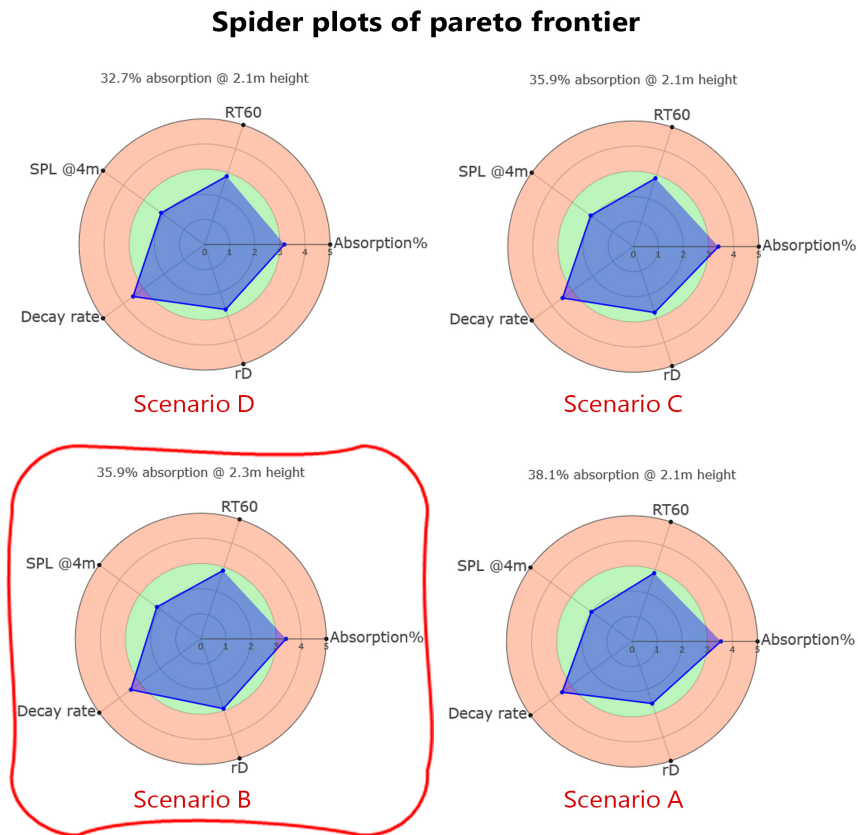


Figure 47: Spider plot analysis of the Pareto scenarios

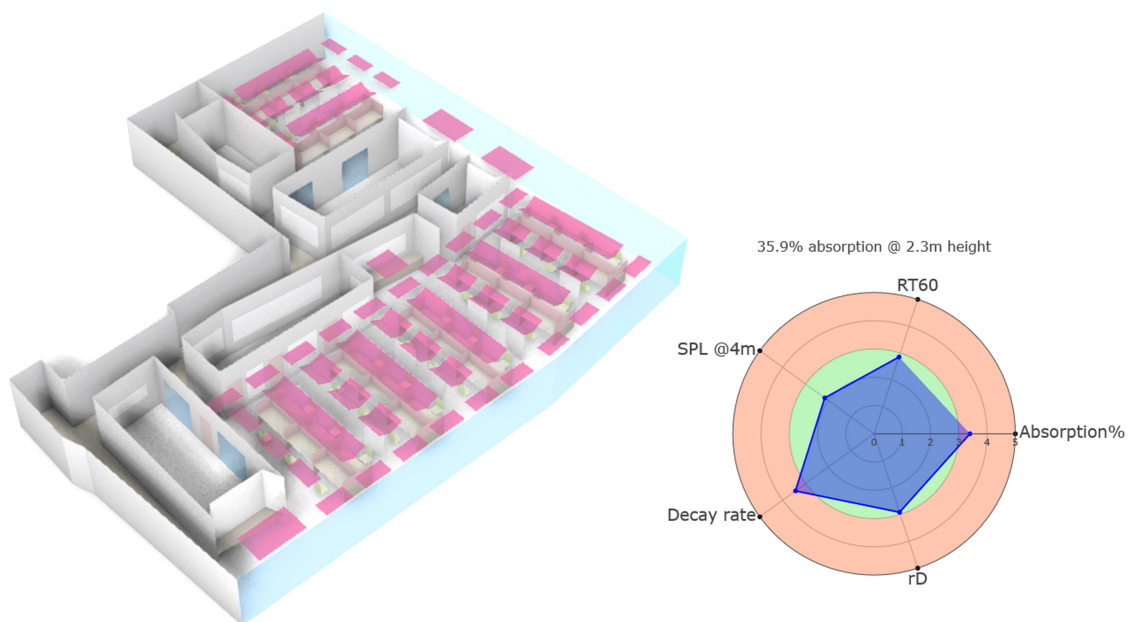


Figure 48: View of the best-case scenario with highlighted HR panel configuration and its spider plot rating

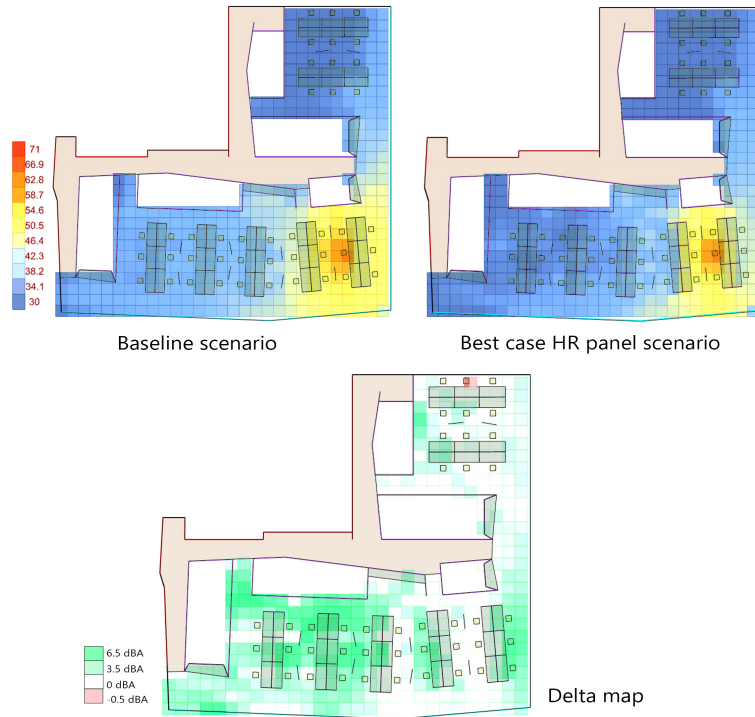


Figure 49: Sound energy distribution in the baseline scenario and the best-case HR panel scenario and their delta map

The sound pressure distribution in the layout from a single source speaker is compared between the two scenarios - the baseline case, and the improved case with HR panels. The best-case scenario performs well in containing the speech sounds from propagating to other workstations when compared to the baseline scenario. This is highlighted in the delta map which shows the energy differences between the two. Green zones, which mark the highest energy difference, are observed one workstation bay away from the speaker with an SPL drop of up to 6.5dBA. The area that is two workstations away from the speaker is completely shielded from the intruding speech sounds. This layout has sufficient buffer spaces that speech originating from one work zone does not percolate into the adjoining workspace. This holds even when there are two simultaneous speakers in each work zone (figure 50). The design of the open office hinders the easy propagation of the sound waves to other zones. When a third speaker is introduced in the corridors, the acoustic quality in the work zones does not deteriorate much due to sufficient screening.

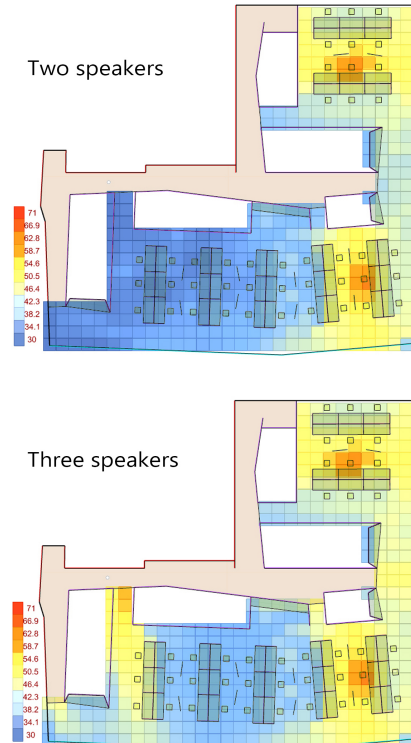


Figure 50: The best-case HR panel scenario with simultaneous speakers

6.3 Office layout 3

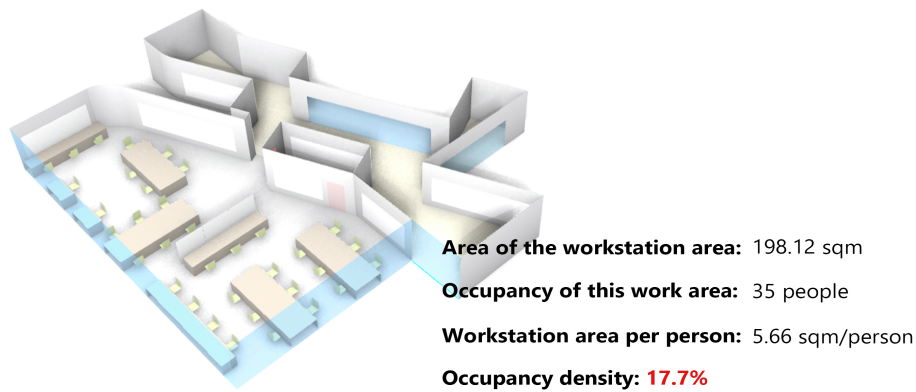


Figure 51: View of office layout 3 and its occupancy density

In layout 3, there are two types of workspaces - collaborative work zones and private work zones. The private work zone is separated from the rest of the circulation zone with just one entry point. Hence, it is visually and acoustically isolated from the public spaces. Pockets of collaborative work zones branch out from the circulation area. The conference and meeting rooms are centralized for access from multiple private work zones while focus and phone rooms are localized and they create an acoustic buffer between the private work zone and the main circulation area. Within the private work zone, groups of 3 to 6 workstations are grouped together without any desk partitions between them. In comparison to the previous case studies, the density is significantly higher, and hence the workstation area per person is smaller.

6.3.1 Baseline scenario

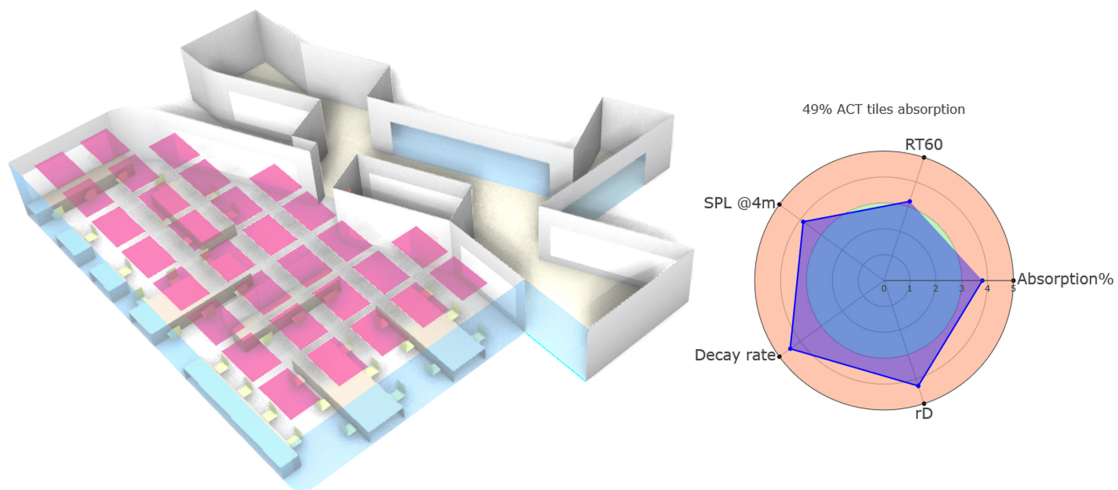


Figure 52: View of the baseline scenario with highlighted acoustic ceiling tiles and its spider plot rating

The baseline scenario of layout 3 is given in figure 52. The highlighted rectangles are porous ceiling tiles adhered to the ceiling, and the ductwork and electrical wiring run in front of these absorbers. 49% of the workstation area is covered by the acoustic ceiling tiles. Apart from these absorbers, there are no other absorptive surfaces in the space—no desk partitions or acoustic liners on the walls. And with the given density of people in the space, all the acoustic parameters fall outside of the ISO’s target range as depicted in the spider chart.

6.3.2 Improvements with HR panels

Two sets of improvements are performed on this layout. Desk partitions of height 0.6m made of fabric encased foam infill are included to improve the sound attenuation in the space (see figure 53). Different tilted HR panel distributions, successively increasing its area, are designed to study the optimum area of absorption required for improving the acoustics. The same height vs. area of absorption matrices are used for studying the trends and each scenario from this matrix is ranked using Pareto front sorting. The area of the panel distributions and the matrices are given in Appendix J. In the Pareto front results (see figure 54), none of the solutions fall within the good acoustics zone marked (green area) in the charts. This can be attributed to the higher occupancy density compared to the other two layouts. For the same reason, the spatial decay values of the candidate scenarios are marginally higher than the values observed in the improved layout 2 and layout 1. Hence, the higher the occupancy density, the larger is the spatial decay (positive influence) and the larger is the distraction distance (negative influence). Though none of the candidate solutions fall within the ISO’s target range, solution A is an acceptable scenario.

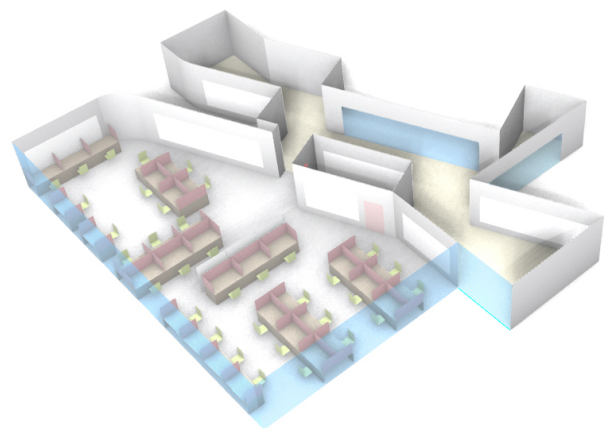


Figure 53: Desk partitions are included to improve the sound attenuation in the open office layout 3

The spider chart acoustic rating of all the candidate solutions are given in figure 55. The candidate solution set include 36.3% @ @2.1m height from the floor (Scenario D), 40.6% @2.1m height (Scenario C), 40.6% @2.3m height (Scenario B), and 46% @ 2.3m height (Scenario A). All the scenarios have satisfactory values in each of the parameters except in distraction distance. Both the spatial decay and the distraction distance improve with increasing area of absorption. So, scenario A which has 46% area of HR panels at 2.3m height from the floor level has a better rating than the acoustic rating achieved in the baseline case. Though the absorber’s area of coverage in scenario A and in the baseline case is similar, scenario A is preferred as it performs well in all the acoustic parameters except in distraction distance.

Pareto front optimization results

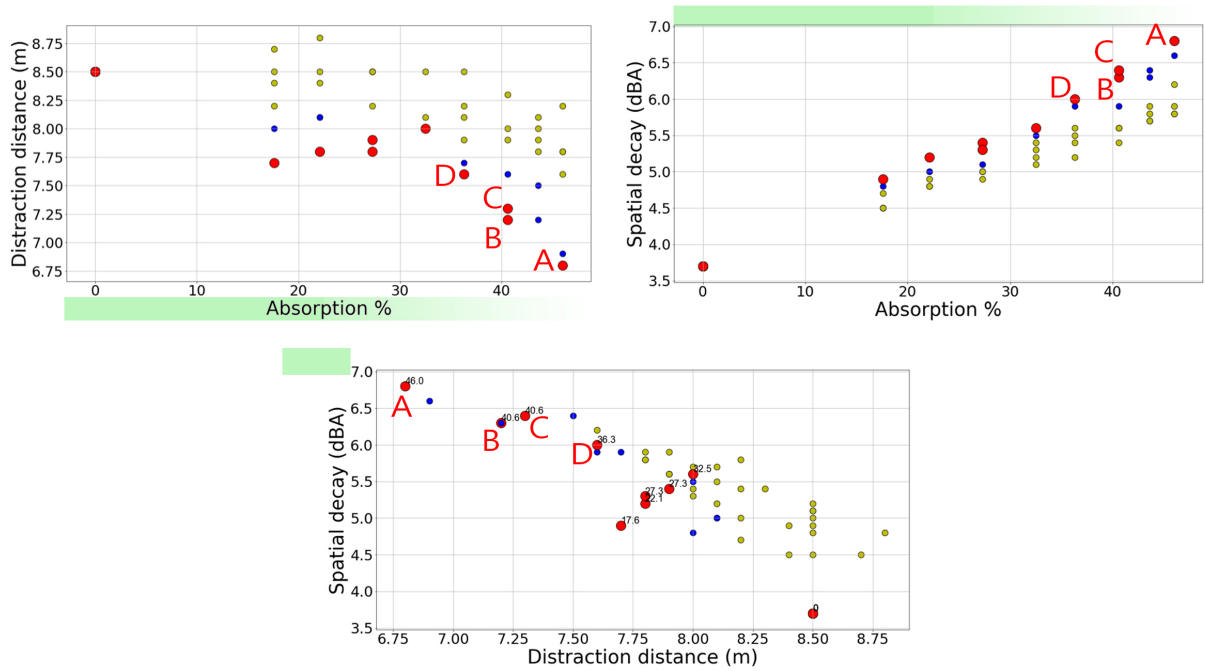


Figure 54: Pareto analysis of the different HR panel configurations

Spider plots of pareto frontier

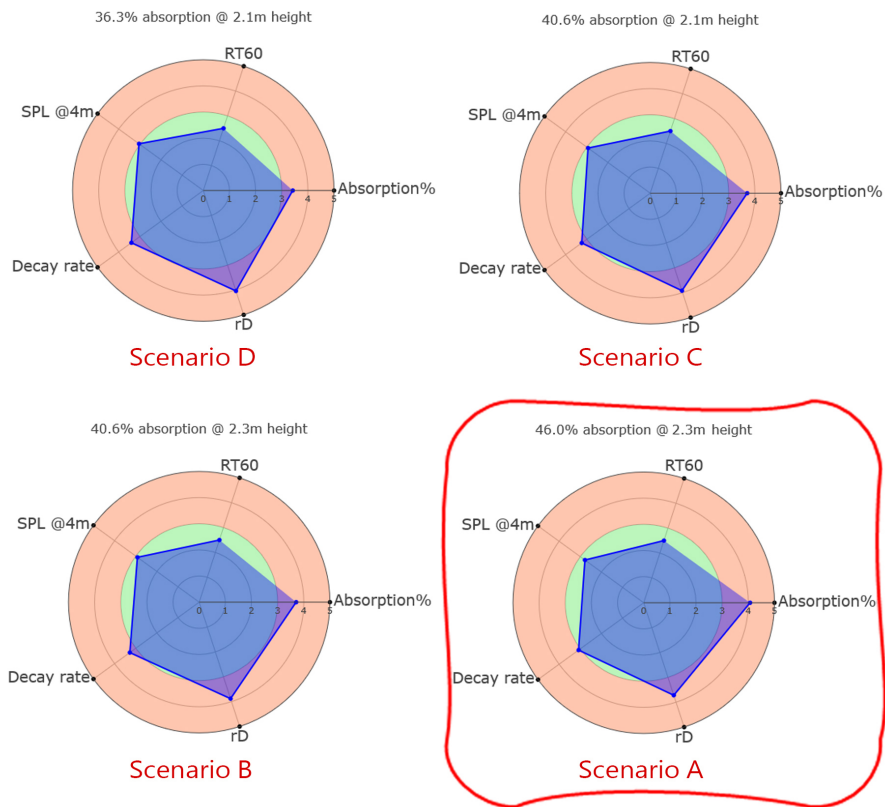


Figure 55: Spider plot analysis of the Pareto scenarios

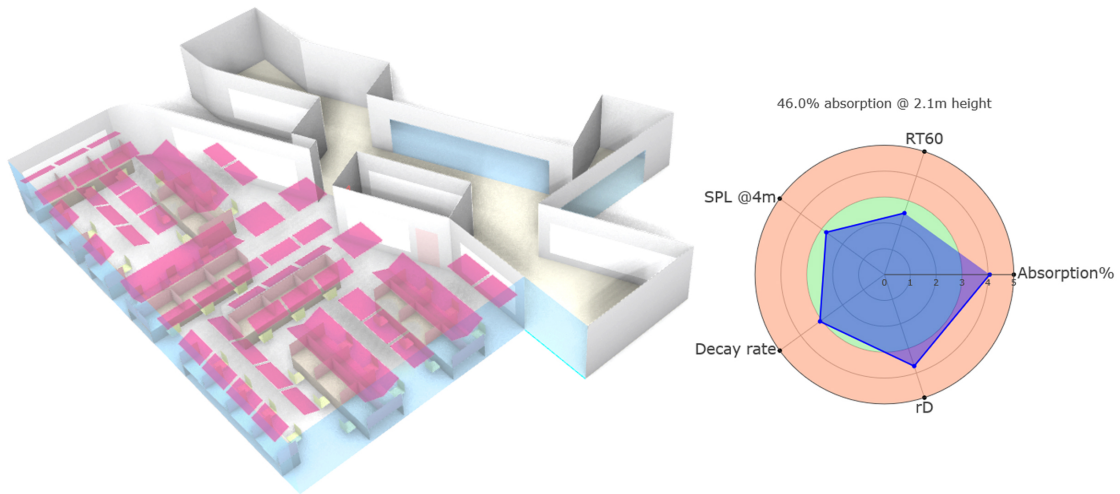


Figure 56: View of the best-case scenario with highlighted HR panel configuration and its spider plot rating

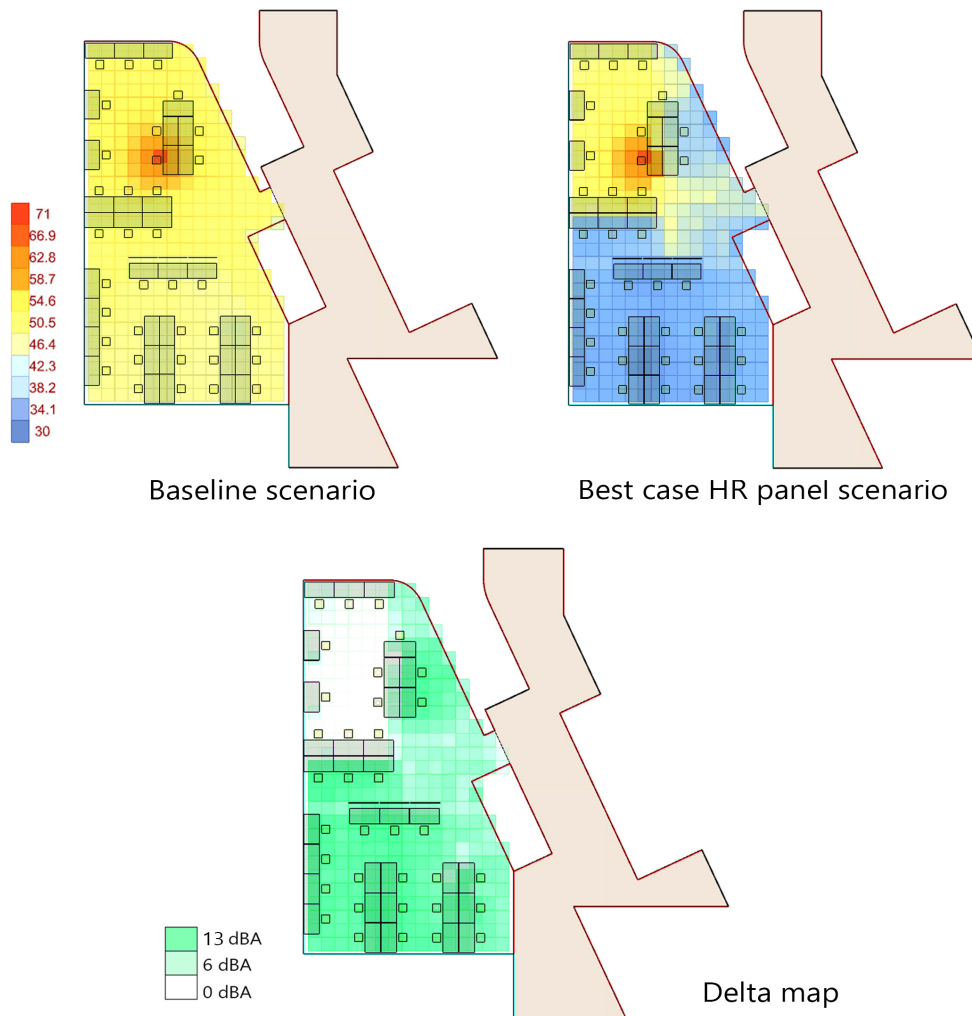


Figure 57: Sound energy distribution in the baseline scenario and the best case HR panel scenario and their delta map

The sound pressure distribution in the layout from a single source speaker is compared between the two scenarios - the baseline case, and the improved case with HR panels and the desk partitions. In the baseline scenario, due to the lack of sufficient absorbers in the space, the sound intensity does not reduce to the comfort levels (depicted by shades of blue in the sound distribution map). In the improved scenario with tilted HR panels, the speech sounds are contained well. The combination of the tilted panels and the desk partitions help in limiting the propagation of sound to the next set of workstations. However, compared to the other two layouts, the number of people affected by a single speaker is more because of the higher occupancy density in this layout. The energy difference between the two scenarios is plotted in the delta map in which the green zone depicts the highest energy difference. Apart from a couple of workstations around the speaker, the rest of the workstations are sufficiently shielded and an SPL drop of up to 13dBA is observed. This is a noticeable difference, as noticeable as not having to sit next to a printer. However, if there are two simultaneous speakers in the improved scenario of this workspace, most of the employees fall in the distraction zone as they are all closely placed (see figure 58). Hence, in the design of the open office, careful consideration of the occupancy density along with the location and amount of absorption is necessary to ensure an acoustically comfortable workspace.

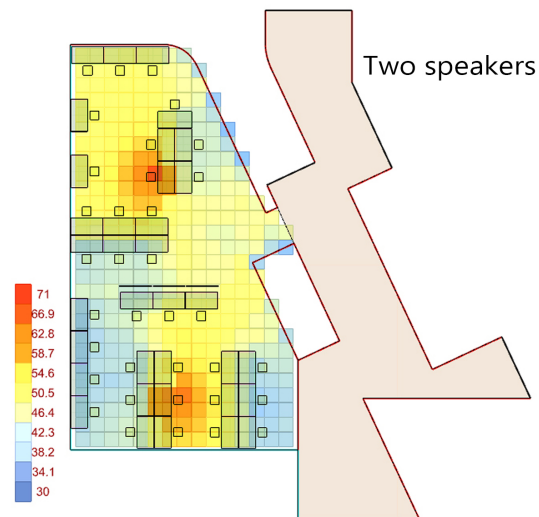


Figure 58: *The best case HR panel scenario with simultaneous speakers*

7 Application Considerations - Materials and Fabrication

7.1 Recycled objects as resonators

Empty plastic bottles (PET bottles) resemble a Helmholtz resonator. The mouth of the bottle acts as the neck of a resonator when left open. Though a wide range of frequencies could not be targeted with these standard-sized bottles, they could be retrofitted to achieve the desired results. A mouthpiece with embedded neck could be fabricated with varying neck lengths to attach to these standard-sized bottles (refer fig 59). This system acts as a resonator with an embedded neck (as described above) and the length of the neck determines the frequency at which the bottle-resonator performs its best. This mouthpiece could also be designed as a conical neck or a perforated neck plate to achieve a variation in the sound frequencies absorbed.

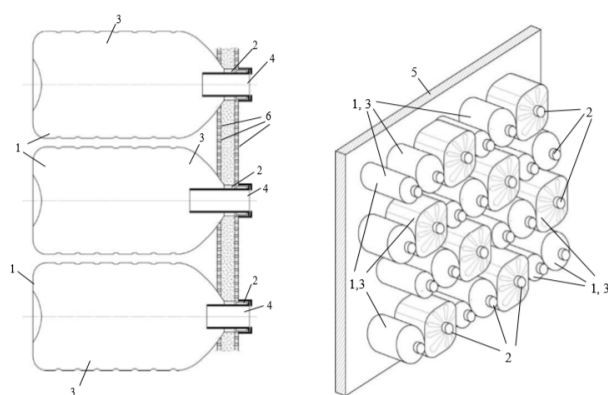


Figure 59: Recycled plastic bottles as a resonator absorber [Fesina et al., 2017]

Scrap wood can be used to mill out a resonator. A resonator made of wood has an added advantage of being a diffusive surface as well. Figure 60 shows a resonator array made of scrap wood. The varying heights of the wood make it a diffuser and the milled out resonator cavity makes it absorptive in the low frequency. The natural voids between the wood resonators act as a quarter-wave resonator (a simple pipe or a tube resonator closed at one end). This broadens the absorption bandwidth of the resonator system. In the same system, another cavity connecting all the milled out cavities is attached to the back end of this system. Hence, each resonator, now, has two connected cavities of air providing the spring effect (called a dual Helmholtz resonator). This improves the sound absorption of the resonator panel.

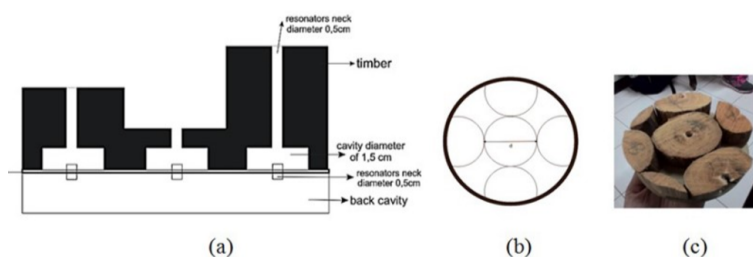


Figure 60: Scrap wood diffuser and absorber [Romadhona et al., 2017]

7.2 Acoustic metamaterials

With the advent of 3D printing technology, more complex geometry for controlling, directing, and manipulating sound waves can be fabricated - called acoustic metamaterials. The precision and customization of geometry achieved with 3D printing have introduced sub-wavelength resonators which are smaller than the wavelength of sound. Sub-wavelength resonators have pioneered developments in compact broadband variants of Helmholtz resonators. An example is depicted in figure 61. It is a spiral metamaterial that is capable of achieving perfect absorption at the resonant frequency. The sound waves are damped in the long winding path embedded with this structure through visco-thermal losses. A panel comprising of coplanar and coiled tubes effectively absorbs low frequency sound with a thickness of less than one percent of wavelength [Cai et al., 2014].

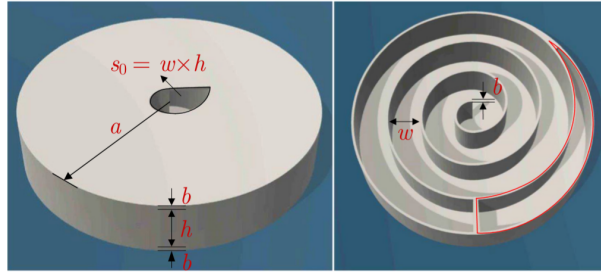


Figure 61: *Spiral sub-wavelength resonator [Huang et al., 2019]*

A traditional Helmholtz resonator's cavity is quite bulky for attenuating low frequencies and has a narrow bandwidth of absorption. And a panel composed of multiple such resonators would be deep and wide which might make them not widely applicable. A sub-wavelength resonator inspired by the dual Helmholtz resonator construct and made possible by 3D printing is given in figure 62. The neck and the first cavity chamber in this split-ring resonator are folded in within the larger cavity, thus saving space without compromising its efficiency. The absorption performance of this resonator and a classical Helmholtz resonator of the same resonant frequency is compared in figure 63.

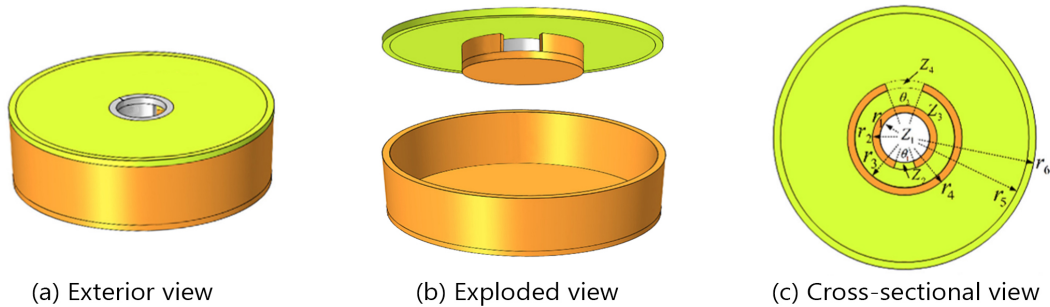


Figure 62: *Sub-wavelength acoustic resonator with split ring neck [Yuan et al., 2019]*

The overall height of the split ring neck resonator designed to achieve the resonant frequency of 196Hz is 22mm and a width of 36mm [Yuan et al., 2019]. The width of the Helmholtz resonator used for comparison is maintained the same. However, to achieve a similar resonant frequency, the neck length is set to 86mm and the cavity depth is 30mm (overall height is 116mm). Hence, for the same resonant frequency, the split ring neck has a better absorption coefficient and a wider bandwidth of absorption at less than one-fifth of the overall height of the Helmholtz resonator. Thus, the sub-wavelength resonators prove to be beneficial in the design and fabrication of a sound absorptive panel composed of resonators. The resonator's performance can be made broader with the inclusion of a thin lossy medium which further improves the visco-thermal losses [Lee et al., 2019].

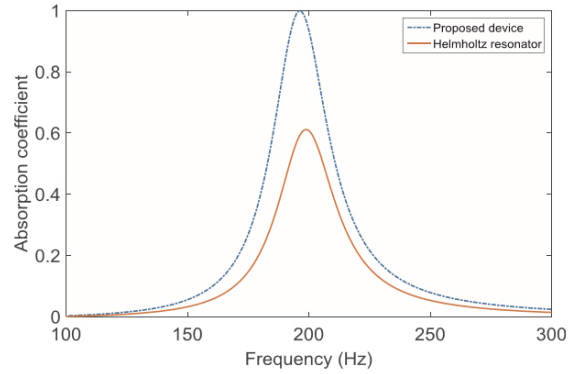


Figure 63: Absorption performance comparison between the split ring neck resonator and a classical Helmholtz resonator [Yuan et al., 2019]

8 Experimentation

To validate the absorption performance of a HR panel obtained analytically, experiments are conducted in an impedance tube setup. ASTM standard test method for impedance and absorption of acoustical materials using two microphones is executed for this experimentation. Though the reverberation room method is an apt method for testing the HR panel's sound absorptive properties, the timeline of this research, fabrication funding, and natural causes (COVID-19 pandemic) thwarted the efforts. The impedance tube method will not be able to test the absorption performance of the whole HR panel discussed in section 4.5 but rather test smaller sections of it. And the results from the impedance tube experiment is only for normal incidence of sound and not for the diffuse sound field which is usually the case in open offices.

The impedance tube method is quite straightforward. A rectangular or circular tube is enclosed on either end with a source and a sample backed by a metal plate. A broadband source produces sound waves that are made planar in the long tube. Microphones are inserted into the walls of the tube to record the forward and backward planar waves to measure the loss in the sound pressure level in the returning waves. The entire setup is made airtight to prevent any leaks and the metal backing plate ensures that the forward planar waves are not transmitted outside. For this research, an impedance tube was custom made to fit the size and shape of the sample and its frequency requirements. The impedance tube was built in collaboration with the Department of Physics at the Central Washington University.

8.1 Construction of the impedance tube

A square cross-section is chosen for the body of the impedance tube to snugly fit the sample piece within it. The walls of the tube are made from 3/4" (0.019m) MDF board and finished with a smooth coating on the interior side to make them non-porous. The interior edge length is 0.2m - derived from a basic working frequency range (F_l to F_u) for this research. The relationship is edge length $< 0.5 * c/F_u$ and accordingly, to have the working frequency flexibility up to 850Hz and to maximize the sample size, the edge length is fixed at 0.2m. Figure 65 shows the construction details of the impedance tube. The length of the main tube is 1.2m long of which 0.6m (or three times the edge length) is the minimum spacing requirement between the source and the microphones to allow for the sound waves to develop into planar waves. The minimum spacing requirement between the microphones and the HR sample (an asymmetrical sample) is two times the edge length. Factoring in all these minimum requirements, the length of the tube is fixed at 1.2m. A smaller length extension is fabricated with the same edge length to house thick samples and to not disrupt the minimum spacing requirements. The ends of the tube have flanges to connect to the tube to different components of the setup. The tube is enclosed on one end with a metal backing plate of 0.02m to reflect back all the on-coming planar waves.

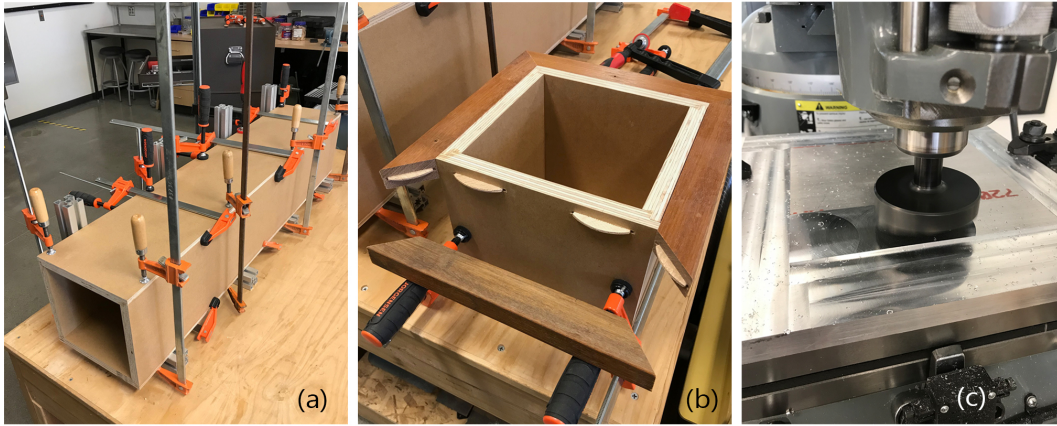


Figure 64: Impedance tube: (a) Square cross-section tube; (b) Flanges at the ends of the tube; (c) Metal backing plate

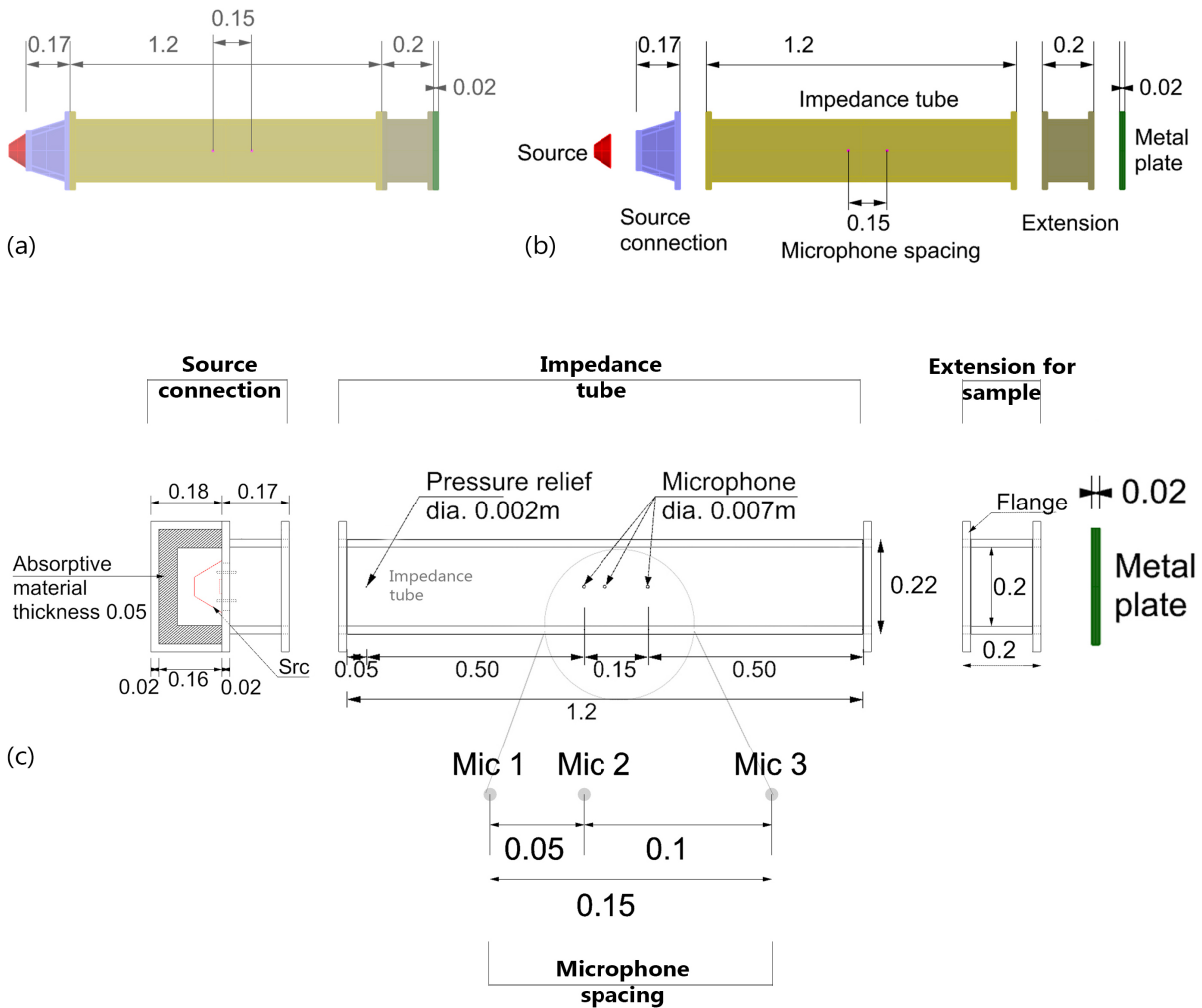


Figure 65: Constructional details of the impedance tube: (a) Conceptual impedance tube setup; (b) Different components of the impedance tube; (c) Detailed section with dimensions of the components

8.1.1 Source and its adapter

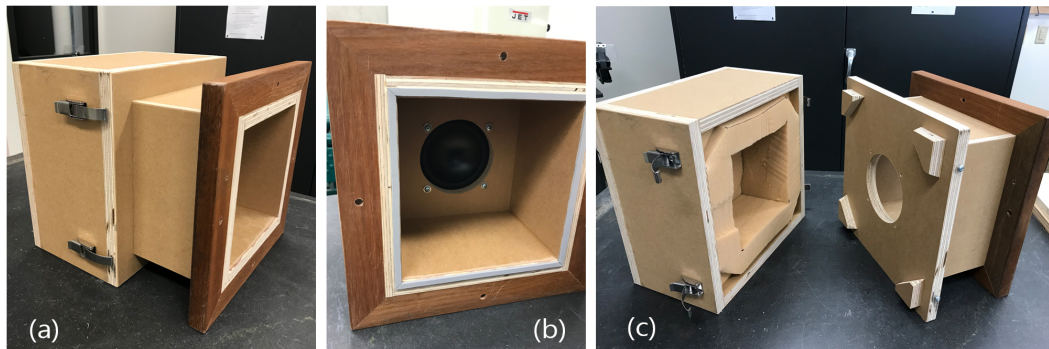


Figure 66: Source connection: (a) View of the source adapter; (b) The adapter's flanges and the thin foam lining around the edges; (c) Foam filled source enclosure

The source is separated from the main impedance tube to reduce the structure-borne sound excitation in the tube. The source adapter has a thin foam lining around the edge of the inner tube for isolation purposes. The source chosen for this experimentation is Dayton Audio ND140-8 5-1/4" driver (0.133m diameter). It has an extended range from 54 Hz to 8 kHz performance. Since it is a direct radiator, it needs an enclosure filled with absorptive material to ensure the airtightness of the tube. The source has an additional extension of about 0.17m (distance from the source location to the adapter's flanges) to further aid in the development of planar waves. A 0.002m hole is drilled into the main tube closer to the source as a pressure relief.

8.1.2 Microphones and their spacing

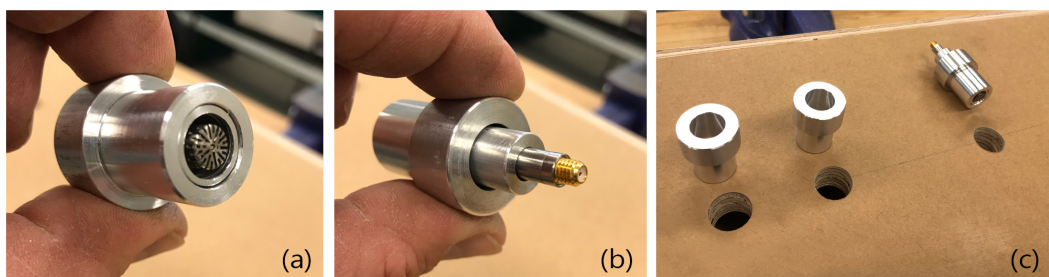


Figure 67: Microphone holder: (a) Front view of the microphone head and its holder; (b) Rear view showing the electrical connection of the microphone; (c) Microphone locations on the main tube

Typically, two microphones are used in this experimentation method and the spacing between the microphones plays a major part in setting the lower limit of the working frequency range. The microphone spacing also affects the quality of the results. Hence, in this impedance tube, three microphones are used to favor both high frequency and low frequency measurements. The maximum microphone spacing is limited to 80% of the upper limit of the working frequency range. Therefore, the distance between the extreme microphones is 0.15m and the third one

is placed at one-third distance from the microphone closest to the source. GRAS 46BD 1/4" (0.007m diameter) microphones are used.

8.1.3 HR panel samples

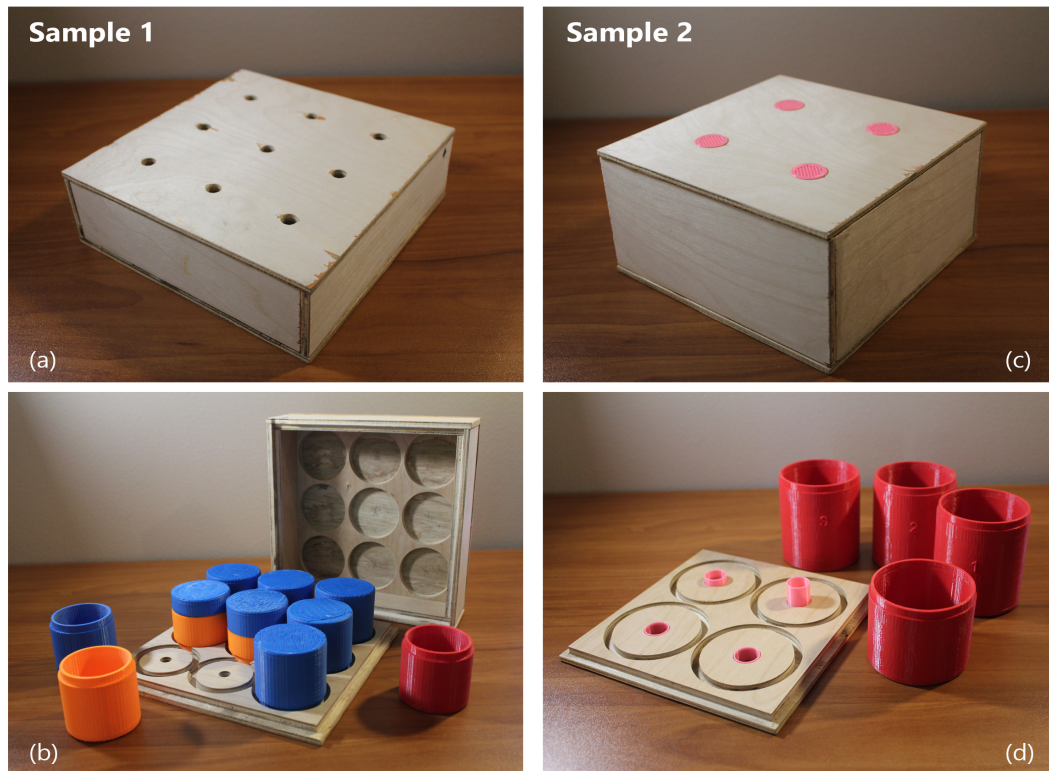


Figure 68: Panel samples: (a) Mid frequency sample 1; (b) Interior view of sample 1; (c) low frequency sample 2; (d) Interior view of sample 2 showing the neck extensions into the cavity

Two sample pieces were fabricated for the experimentation - Sample 1 has resonators working in the mid frequencies, and Sample 2 has large resonators for low frequencies. The resonators were 3D printed and the encasing box was milled out of plywood. In both the samples, the resonators are embedded into the top and bottom plywood plates through friction which ensures airtightness and allows for interchangeability. The top plates are removable to allow the switching of resonators. In sample 1, the resonators are sized to achieve peak absorption at mid frequencies and the necks are drilled into the 1/2" (0.013m) top plate. The relatively small size of the resonators allows nine resonators to be fitted with a 0.2m x 0.2m panel. Since the resonators are replaceable, in one iteration, all the resonators are identical to validate the correctness of the resonant frequency calculation. In another iteration, just one resonator is replaced with a dissimilar resonator to validate the mutual interaction between varying resonators. Since Kim's mutual impedance equation does not account for the arrangement of the resonators, the dissimilar resonator in the sample panel is moved around to verify the impact of arrangement on the absorption performance of the array.

Sample 2 is built for testing a low frequency panel, and hence the resonators used have bigger cavities. Compared to sample 1, sample 2 has a lesser number of resonators and is deeper to accommodate the low frequency resonators. In the simple case, the resonators are attached to the top plate without any neck attachments, to verify the analytical formulas. In the next iteration, hollow-neck attachments are inserted into the neck to model the embedded resonator type (discussed in section 3.2) which further reduces the resonant frequencies. In the final iteration, the hollow neck attachments are swapped with perforated neck attachments of the same length to widen the bandwidth of absorption. All the cases are compared to analyze the improvements in the absorption performance as observed in the analytical results.

8.1.4 Completed impedance tube setup



Figure 69: View of the completed impedance tube setup

Figure 69 shows the completed impedance tube setup ready for calibration. All the flanges used for connecting the different components are maintained at the same height and hence are used as supports to prop up the setup. This is placed on a shock absorber mat to reduce any interference from external vibrations. The possible areas of error accumulation in this setup include air leaks around joints, gaps between the tube and the mounted sample, increased pressure in the tube after sample mounting which might disrupt the microphone measurements, and structural vibrations from the source during the measurements.

8.2 Experiment results

The experimentation results were recorded using the LabVIEW software and post-processed in MATLAB. On the recorded data, Fast Fourier Transformation (FFT) and transfer functions were applied to convert the electrical measurements into absorption performance curves. Further details of this process can be found in the ASTM standards.

8.2.1 Experiment set 1

In set 1, two configurations of sample 1 were measured. In the first configuration, all the resonators were maintained identical and in the second configurations, just one of the resonators

was replaced with a dissimilar resonator. This was done to measure the difference that one dissimilar resonator can make. The results are given in figure 70. The red line shows the results from analytical predictions and the blue line denotes the experimentation results.

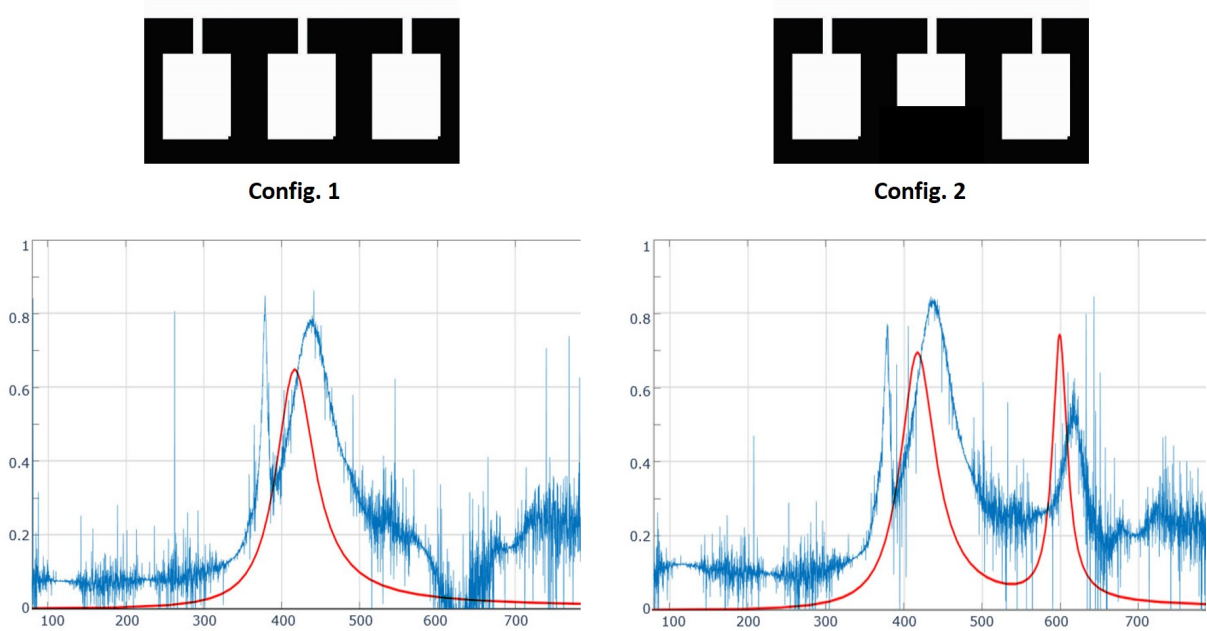


Figure 70: The configurations used in experiment set 1 and their corresponding absorption performances—overlapped experiment results and analytical predictions

Overall, there is a good agreement between the analytical predictions and the experiment results. A shift is observed between the two results which could have been caused due to imperfections in the fabrication and the placement of the sample in the impedance tube. The measured values are also slightly higher than the predicted values which might be because of the absorptive properties of the sample’s top plate. In configuration 1, there is just one prominent spike in the absorption performance curve because all the resonators are identical. While in configuration 2, with just one dissimilar resonator, another spike corresponding to the resonant frequency of the dissimilar resonator is observed. However, the height of that spike is not as high as the prediction. The mutual interaction between the resonators can be observed in the valley between the two spikes. The experiment results show a better mutual interaction than the predicted behavior.

8.2.2 Experiment set 2

In set 2, three configurations by changing the relative position of the dissimilar resonator in sample 1 were measured to observe the variations induced by the arrangement of resonators. The results are given in figure 71. The red line shows the results from the analytical predictions and the blue, green, and deep-orange lines correspond to configurations 1, 2, and 3, respectively. Figure 71 shows the overlapped performances of configuration 1 and 2, and all

the configurations. There is a marginal difference between the absorption performances of the three configurations. Hence, Kim’s mutual impedance equation which does not account for the arrangement of the resonators is a reasonable abstraction to calculate the absorption performance of an array of resonators. However, sufficient experimentation would have to be done on a larger panel of resonators to confirm the independence of the mutual impedance equation from the relative positions of the resonators.

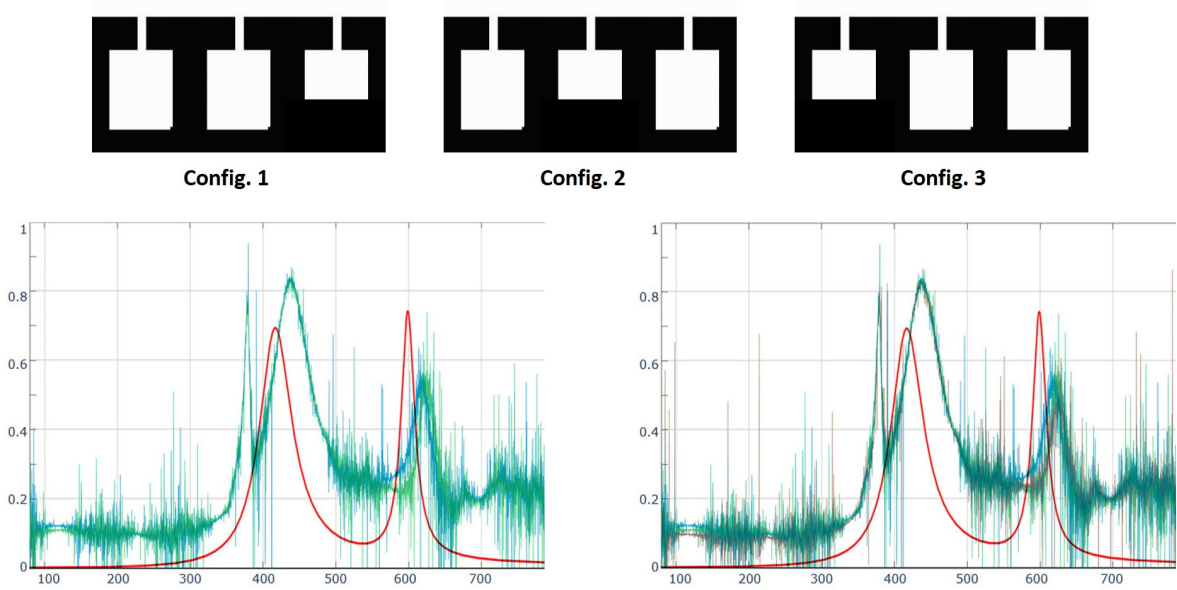


Figure 71: The configurations used in experiment set 2, and the overlapped absorption performances of configuration 1 and 2, and all the configurations

8.2.3 Experiment set 3

This set uses sample 2 to test the efficiency and the accuracy in the predicted performances of embedded neck resonators. Hollow 3D printed necks of varying lengths can be inserted into the top plate of the sample without changing the resonators. Accordingly, configuration 1 does not have any embedded necks (thus, a simple resonator geometry) and configuration 2 has hollow necks embedded into the resonators to compare the performances of both. Figure 72 shows the experiment results of both the configurations overlaid with the results from the analytical predictions (depicted through red lines). In configuration 1, though there are four resonators, the resonant frequencies are clumped together to form two spikes in the performance graph. These spikes are between 330Hz - 400Hz. While in configuration 2, the embedded necks lower the resonant frequencies of the resonators to below 350 Hz. And four prominent spikes can be observed in its performance graph as the lengths of the embedded necks are all different. The 200Hz spike corresponds to the resonator with the longest embedded neck.

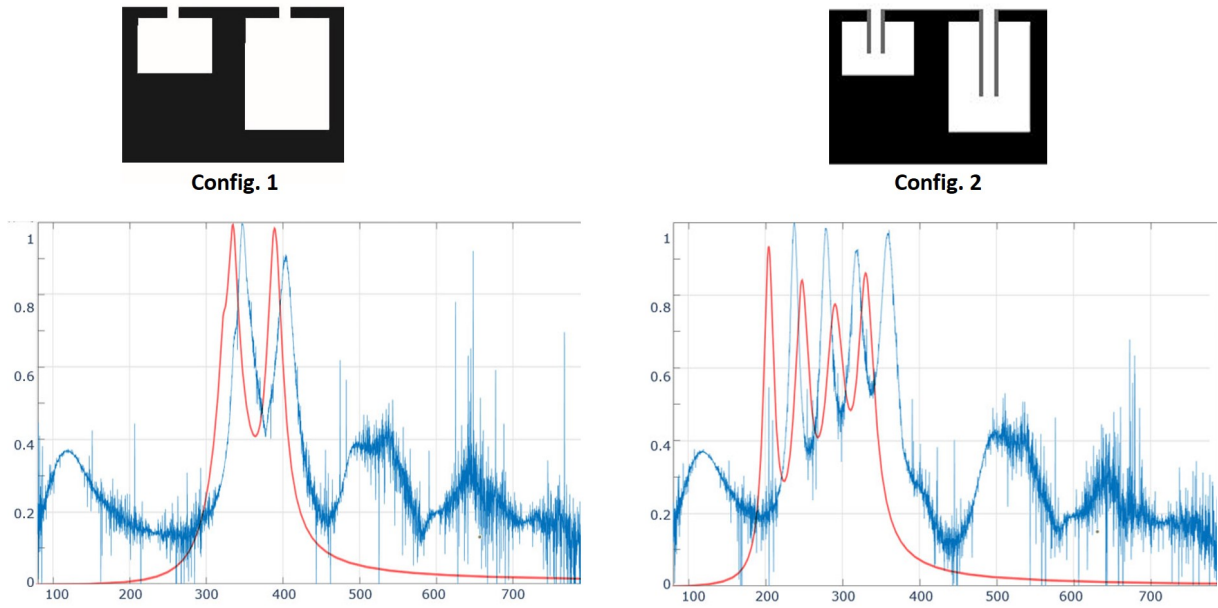


Figure 72: The configurations used in experiment set 3 and their corresponding absorption performances—overlapped experiment results and analytical predictions

Again, a shift is observed between the experiment results and the analytical predictions. In configuration 1, the shift is small and could be due to the imprecision in fabrication. However, the shift observed in configuration 2 is relatively large and could be due to a combination of inaccuracies in fabrication and abstractions used in the analytical formulas. Also, the peak absorption values in the experiment results are higher than the predicted peak values.

8.2.4 Experiment set 4

In set 4, two variants of the embedded necks are explored in the sample 2. In configuration 1, hollow necks are embedded into the resonators and in the other configuration, the hollow necks are replaced with neck perforations of the same length to model additional resistance in the necks. The neck perforations have 48 cylindrical voids of diameter 2mm that run throughout the length of the embedded neck. Hence, the neck perforations are 48% porous and are completely 3D printed. Figure 73 shows the comparison between the performances of the two neck variants. In configuration 1, the resonant frequencies of the resonators are predicted to be in the range 200Hz - 330Hz, but the experiment results exhibit a range of 230Hz - 360Hz. This 30Hz shift could be due to error accumulation in fabrication or in the analytical formulas used. In configuration 2, the predicted resonant frequencies fall in the range 150Hz - 250Hz and it matches well with the experiment results. The analytical formulas used are precise in the predictions. Although the resonant frequencies match, the peak values are lower in the experiment results in comparison to the predictions. This could be due to imperfections in the 3D printing of the neck perforations as the opening size of the pores are small.

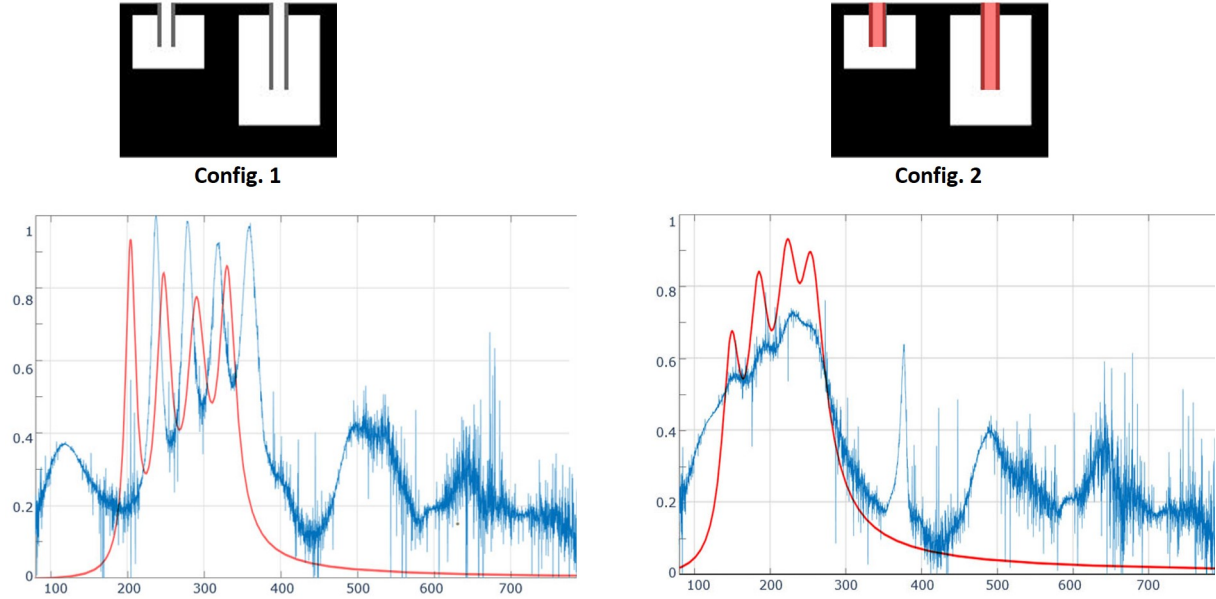


Figure 73: *The configurations used in experiment set 4 and their corresponding absorption performances—overlapped experiment results and analytical predictions*

The neck perforations (or additional resistance in the necks) have a twofold advantage - they lower the resonant frequencies and they improve the absorption performance in the valleys between the resonant peaks. However, due to fabrication constraints, the resonant peaks are not prominent in the experiment results. But the improvements in the valleys are noticeable in the configuration 2 graph in figure 73.

8.2.5 Limitations

Overall, the experiment results agree well with the analytical predictions. However, it has to be noted that the calibration step involved before the measurements were taken in the impedance tube, was not accurately done. The calibration and the phase correction of the microphones are done with an absorptive foam wedge on one end of the tube instead of the reflective metal plate. In our calibration step, the foam wedge was not sufficiently absorptive and hence caused low frequency roll-off and messiness in the frequency range above 900Hz. So, this step was skipped in all the measurements taken. But these experiment results are reliable as the microphones used are precise and have a very low offset percentage.

Another consistent limitation observed in the experiment results is a sharp projection around 380Hz. This could have been caused by the resonance of the impedance tube which acts as a quarter wavelength resonator. The sharp projection can be avoided with the calibration step. In general, the calibration step helps in removing the environment-dependent inconsistencies—the resonance of the impedance tube and the phase differences in the microphones. The calibration step will be re-worked and added to the measurements for the upcoming research paper publications.

9 Conclusions and discussion

Through this research, the potential application of Helmholtz Resonators in an open office is explored. Resonator panels are a "healthier" and a competent solution in improving the open office acoustics. Focus on reducing the annoyance caused by low frequencies and the intruding speech signals are the major driving forces in the resonator panel design. And the panel's application in room acoustic simulations proved to be beneficial over acoustic ceiling tiles.

In the Helmholtz Resonator scale, the basic resonator geometry and a couple of simple modifications to that geometry were analyzed. With these geometries, resonators were designed to specifically attenuate the frequencies important for speech intelligibility. Resonators designed for the low frequencies were large and they take up a lot of space. However, acoustic meta-materials, made possible through 3D printing, have complex resonator geometry that is more compact and can achieve perfect absorption in low frequencies. Such complex geometries do not have an existing analytical method to derive their absorption performance. Still, they can be studied using Finite Element Analysis (FEA) simulations.

In the array of resonators scale, the coupling effect between the resonators gave the resonator panel a competitive advantage over porous absorbers. The spacing between the resonators is an important parameter that controls the positive impact of mutual interaction between the resonators. And with large low frequency resonators in the panel, the compactness and the absorption performance of the panel diminishes. However, replacing the traditional resonators with the more advanced sub-wavelength resonators might solve this problem.

In the room-scale, geometrical acoustic simulations were run for studying the effectiveness of HR panels in open offices. Three case studies were chosen to compare the results from its baseline case and from an improved case with HR panels. Tilted ceiling-hung HR panels attained good acoustics for a smaller absorption area coverage when compared to the acoustic ceiling tiles used in the baseline case. However, these results are not representative of the actual situation as the simulation models do not factor in edge diffraction, sound interference, or room modes. Studying the trends helped focus on the location optimization of the absorbers in the open office.

The experimentation helped bridge the results from analytical predictions and physical testing, and understand the limitations in both the procedures. Though the reverberation chamber method would have provided a thorough understanding of the panel's behavior in room conditions, the impedance tube method helped test out a number of iterations of the samples with minimum fabrication and calibration of the setup. The results from an impedance tube experiment can help in calibrating an FEA model when analyzing complex resonator geometry.

Though the resonator panel designed in this project is bulky and might not prove to be practical, it provides a starting point to analyze the usefulness of Helmholtz Resonators in room acoustics. Instead of having the resonators in a ceiling-hung panel, these could even be integrated into the ceiling slab design or in the partition walls and could become an integral aspect for improving room acoustics.

9.1 Future work



Figure 74: Resonators from everyday objects: (a) Cardboard tubes; (b) Plastic bottles; (c) Bamboo shoots

The next steps in continuing this research would be targeted towards complex resonator geometry that is more compact and broadband in their performance like the sub-wavelength resonators discussed in section 7.2. Hence, a shift towards FEA simulations is required as the boundaries of analytical models have been met with this research. On the array scale, an in-depth study on the impact of the resonator arrangement on the absorption performance of the panel is of interest.

Figure 74 shows some of the recyclable objects (plastic bottles and cardboard tubes) and naturally occurring material, like bamboo shoots, that can be used as resonators. They might prove to be more eco-friendly and carbon-neutral when compared to other synthetic materials for fabricating the resonators. Further research would have to be conducted to bolster the application and advantages of these materials as efficient resonators.

The application of the resonator panel in spaces other than open offices is an interesting direction. Since the resonators are relatively dust-free compared to porous absorbers, they could be used in sensitive rooms in a hospital. Research on integrating them into building components - like partition walls or ceiling slabs - could provide novel ways in designing spaces for acoustic comfort.

10 Appendices

10.1 Appendix A - Helmholtz resonator's performance calculator

An interface was built using python in Jupyter notebook and libraries, such as Plotly and ipywidgets. Plotly is a python library for generating interactive graphs and charts. Ipywidgets is used for receiving user inputs in the form of text or option from a list of choices. Figure 76 shows the interface to compute the sound absorption of different geometrical configurations of Helmholtz resonators. The calculator is built on the formulas discussed in section 3.3 for the various resonator designs. The user is expected to choose a type of resonator geometry and feed the geometry values in the given text boxes. As the user changes these geometry values, the resonant frequency, and the sectional representation of the resonator are automatically updated. The user also has the option to choose one of the additional neck resistances as discussed in section 3.4. The “Generate graph” button produces the absorption performance curve of the resonator over the frequency range specified in the code. Performance comparison can be made between a resonator with and without the additional resistance.

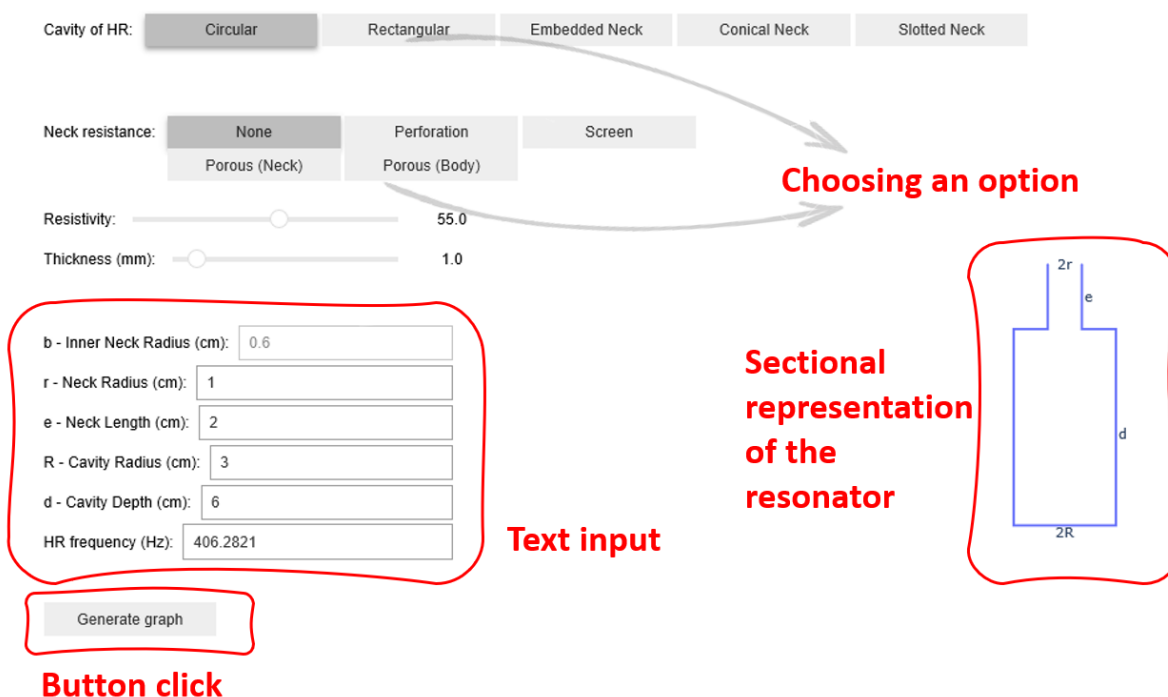


Figure 75: Inputs required to run the calculator

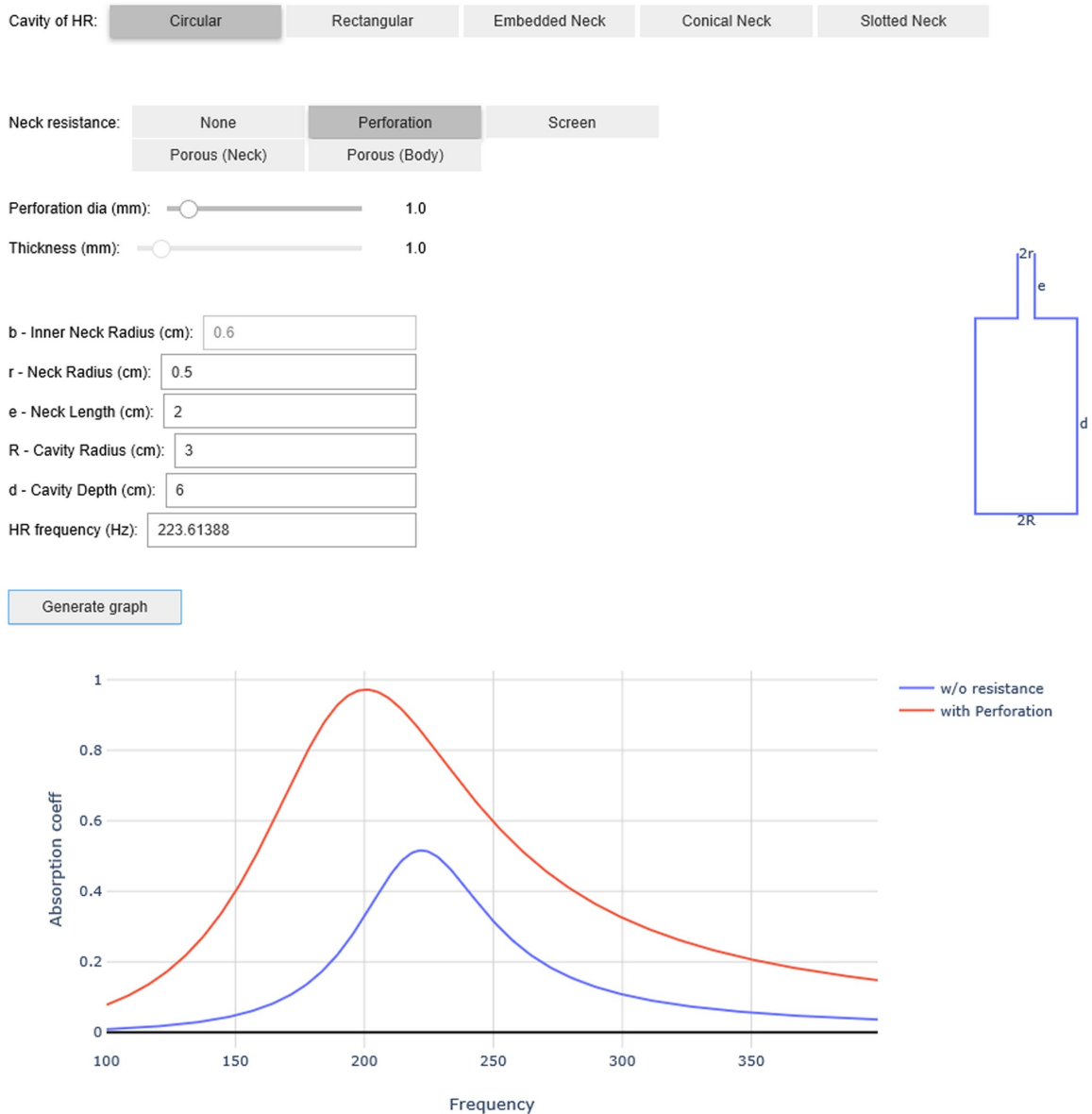


Figure 76: Interface for calculating the sound absorption of different kinds of Helmholtz resonators

10.2 Appendix B - Semi-automated resonator array calculator

A simple interface was built to semi-automate the process of the resonator array design which requires minimum input from the users. The user is expected to provide the bandwidth of absorption that they are interested in and the closeness of the resonance peaks (refer figure 77). This decides the number of resonators in the panels and their resonant frequencies. The user can choose a panel type composed of one out of the three cases discussed in section 4.2 - Cylindrical cavity, Square cavity, and Embedded neck cylindrical cavity (refer figure 78) and control the panel's depth. Based on the resonator geometry, the user can also specify the neck length for maintaining it constant. The neck radius and spacing between the resonators are fixed variables and are defined in the python code.

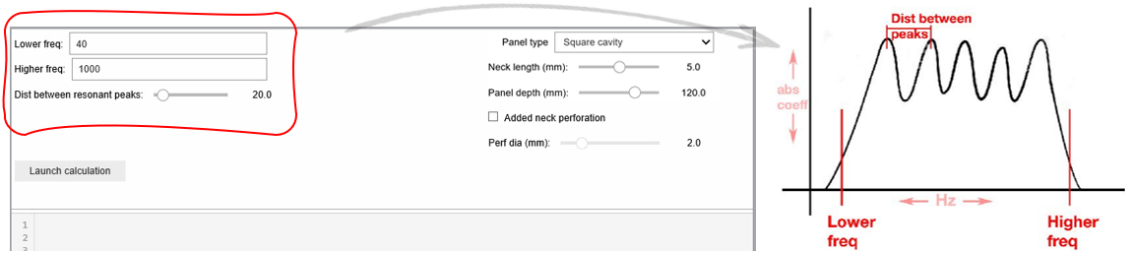


Figure 77: Inputs: Frequency bandwidth and the closeness of the resonant frequencies

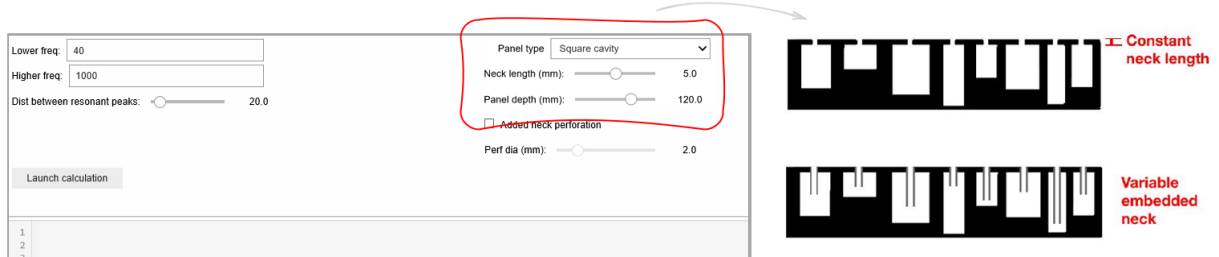


Figure 78: Input: Panel type

Additional neck resistance to improve the absorption performance can be added by checking the box in the interface (refer figure 79). Currently, the additional resistance is provided in the form of perforated neck plates. The user can specify the pore size of the perforations.

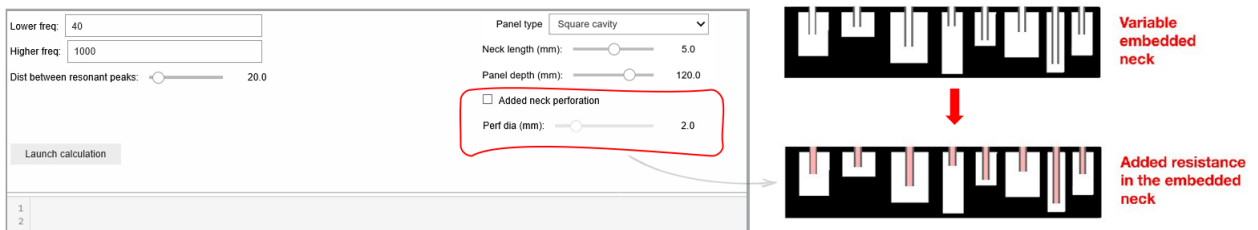


Figure 79: Checkbox to include additional neck resistance

10.3 Appendix C - Open office acoustic simulations

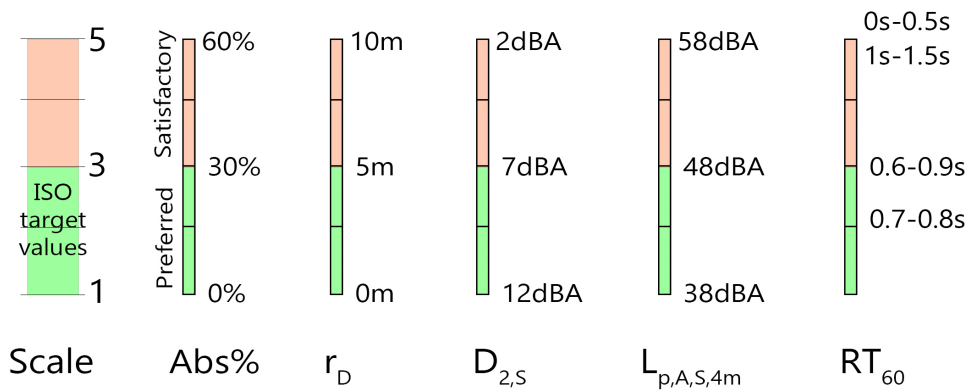


Figure 80: Conversion of single-number parameter ranges to polar scale metrics

Rhino element	Material	Absorption coefficients							
		63Hz	125Hz	250Hz	500Hz	1000Hz	2000Hz	4000Hz	8000Hz
Walls	2x13mm plasterboard on steel frame, 5cm mineral wool in the cavity, surface painted	0.17	0.15	0.1	0.06	0.04	0.04	0.05	0.06
Wall treatment	Fabric tiles	0.03	0.03	0.2	0.3	0.3	0.27	0.19	0.12
Windows	Large pane heavy glass	0.22	0.18	0.06	0.04	0.03	0.02	0.02	0.02
Flooring	Vinyl flooring	0.03	0.04	0.04	0.07	0.06	0.06	0.07	0.07
Corridor	6mm carpet on foam lining	0.03	0.03	0.09	0.25	0.31	0.33	0.44	0.44
Ceiling	Smooth concrete	0.01	0.01	0.01	0.02	0.02	0.02	0.05	0.04
Furniture	Wooden	0.12	0.12	0.12	0.13	0.13	0.1	0.1	0.1
Furn - Table	Wooden table top	0.1	0.15	0.19	0.22	0.39	0.38	0.3	0.25
Furn - Chair	Chair	0.15	0.22	0.28	0.32	0.35	0.32	0.28	0.22
Desk partition	Fabric + foam	0.04	0.19	0.3	0.36	0.52	0.79	0.86	0.73
Ceiling-hung panel	Helmholtz resonator panel	0.35	0.73	0.83	0.93	0.94	0.35	0.3	0.1

Figure 81: Absorption coefficients used in the Rhino model for the acoustic simulation

Rhino element	Material	Absorption coefficients							
		63Hz	125Hz	250Hz	500Hz	1000Hz	2000Hz	4000Hz	8000Hz
Ceiling-hung panel	Helmholtz resonator panel	0.35	0.73	0.83	0.93	0.94	0.35	0.3	0.1
	Mineral fiber acoustic tile	0.15	0.35	0.34	0.48	0.69	0.88	0.92	0.87

Figure 82: Absorption coefficients used Study 1

References

- [Abbaszadeh et al., 2006] Abbaszadeh, S., Zagreus, L., Lehrer, D., and Huizenga, C. (2006). Occupant satisfaction with indoor environmental quality in green buildings.
- [Bradley, 2004] Bradley, J. (2004). *Acoustical design for open-plan offices*. Institute for Research in Construction, National Research Council of Canada.
- [Bradley, 2003] Bradley, J. S. (2003). The acoustical design of conventional open plan offices. *Canadian Acoustics*, 31(2):23–31.
- [Brennan et al., 2002] Brennan, A., Chugh, J. S., and Kline, T. (2002). Traditional versus open office design: A longitudinal field study. *Environment and behavior*, 34(3):279–299.
- [Cai et al., 2014] Cai, X., Guo, Q., Hu, G., and Yang, J. (2014). Ultrathin low-frequency sound absorbing panels based on coplanar spiral tubes or coplanar helmholtz resonators. *Applied Physics Letters*, 105(12):121901.
- [Carvalho De Sousa et al., 2019] Carvalho De Sousa, A., Deckers, E., Claeys, C., and Desmet, W. (2019). Parallel assembly of acoustic resonators to obtain narrow-band unity sound absorption peaks below 1000 hz. <http://www.icedyn.net/>.
- [Cox and d’Antonio, 2016] Cox, T. and d’Antonio, P. (2016). *Acoustic absorbers and diffusers: theory, design and application*. Crc Press.
- [cyberstates.org, 2020] cyberstates.org (2020). The definitive guide to the u.s. tech industry and tech workforce.
- [Davidsson, 2016] Davidsson, F. (2016). Generating and understanding speech.
- [Delle Macchie et al., 2018] Delle Macchie, S., Secchi, S., and Cellai, G. (2018). Acoustic issues in open plan offices: A typological analysis. *Buildings*, 8(11):161.
- [Ebissou et al., 2015] Ebissou, A., Parizet, E., and Chevret, P. (2015). Use of the speech transmission index for the assessment of sound annoyance in open-plan offices. *Applied Acoustics*, 88:90–95.
- [Fesina et al., 2017] Fesina, M. I., Krasnov, A. V., and Gorina, L. N. (2017). On different engineering ideas of eco-designer resource-saving studies of effective sound-absorbing substances and noise-reducing constructions. *Procedia Engineering*, 176:150–158.
- [Fuchs, 2013] Fuchs, H. V. (2013). *Applied Acoustics: Concepts, Absorbers, and Silencers for Acoustical Comfort and Noise Control: Alternative Solutions-Innovative Tools-Practical Examples*. Springer Science & Business Media.
- [Gommer, 2016] Gommer, B. (2016). Resistance in helmholtz resonators: Exploring the potential of sound absorption created by additive manufacturing.

- [Griffin et al., 2000] Griffin, S., Lane, S. A., and Huybrechts, S. (2000). Coupled helmholtz resonators for acoustic attenuation. *J. Vib. Acoust.*, 123(1):11–17.
- [Haapakangas et al., 2017] Haapakangas, A., Hongisto, V., Eerola, M., and Kuusisto, T. (2017). Distraction distance and perceived disturbance by noise—an analysis of 21 open-plan offices. *The Journal of the Acoustical Society of America*, 141(1):127–136.
- [Hodgson, 2011] Hodgson, M. (2011). Evaluation and control of acoustical environments in ‘green’(sustainable) office buildings. *Canadian Acoustics*, 39(1):11–21.
- [Huang et al., 2019] Huang, S., Fang, X., Wang, X., Assouar, B., Cheng, Q., and Li, Y. (2019). Acoustic perfect absorbers via helmholtz resonators with embedded apertures. *The Journal of the Acoustical Society of America*, 145(1):254–262.
- [ISO 3382-3, 2012] ISO 3382-3 (2012). Acoustics - Measurement of room acoustic parameters - Part 3: Open-plan offices.
- [Johansson and Kleiner, 2001] Johansson, T. A. and Kleiner, M. (2001). Theory and experiments on the coupling of two helmholtz resonators. *The Journal of the Acoustical Society of America*, 110(3):1315–1328.
- [Jordan, 1947] Jordan, V. L. (1947). The application of helmholtz resonators to sound-absorbing structures. *The Journal of the Acoustical Society of America*, 19(6):972–981.
- [Keränen et al., 2008] Keränen, J., Virjonen, P., Elorza, D. O., and Hongisto, V. (2008). Design of room acoustics for open offices. *SJWEH Supplements*, (4):46–49.
- [Kim, 2010] Kim, Y.-H. (2010). *Sound propagation: an impedance based approach*. John Wiley & Sons.
- [Lee et al., 2019] Lee, T., Nomura, T., and Iizuka, H. (2019). Damped resonance for broadband acoustic absorption in one-port and two-port systems. *Scientific reports*, 9(1):1–11.
- [Lee and Kim, 2008] Lee, Y. S. and Kim, S.-K. (2008). Indoor environmental quality in leed-certified buildings in the us. *Journal of Asian Architecture and Building Engineering*, 7(2):293–300.
- [Leventhall et al., 2004] Leventhall, H. G. et al. (2004). Low frequency noise and annoyance. *Noise and Health*, 6(23):59.
- [Nilsson and Hellström, 2010] Nilsson, E. and Hellström, B. (2010). Nt technical report.
- [Pierre Jr et al., 2004] Pierre Jr, R. L. S., Maguire, D. J., and Automotive, C. S. (2004). The impact of a-weighting sound pressure level measurements during the evaluation of noise exposure. In *Conference NOISE-CON*, pages 12–14.

- [Polychronopoulos et al., 2014] Polychronopoulos, S., Skarlatos, D., and Mourjopoulos, J. (2014). Efficient filter-based model for resonator panel absorbers. *Journal of the Audio Engineering Society*, 62(1/2):14–24.
- [Rindel, 2011] Rindel, J. H. (2011). Echo problems in ancient theatres and a comment to the ‘sounding vessels’ described by Vitruvius. In *Proc. The acoustics of ancient theatres Conference, Patras*.
- [Rindel, 2018] Rindel, J. H. (2018). Open plan office acoustics—a multidimensional optimization problem. *Proceedings of DAGA2018, Munich, Deutsche Gesellschaft für Akustik*.
- [Romadhona et al., 2017] Romadhona, I. C., Yahya, I., et al. (2017). On the use of coupled cavity Helmholtz resonator inclusion for improving absorption performance of wooden sound diffuser element. *Procedia engineering*, 170:458–462.
- [Schlittmeier and Liebl, 2015] Schlittmeier, S. J. and Liebl, A. (2015). The effects of intelligible irrelevant background speech in offices—cognitive disturbance, annoyance, and solutions. *Facilities*.
- [Selamet and Lee, 2003] Selamet, A. and Lee, I. (2003). Helmholtz resonator with extended neck. *The Journal of the Acoustical Society of America*, 113(4):1975–1985.
- [Van der Aa, 2012] Van der Aa, B. (2012). Ground buried resonators analytical and numerical modelling of their noise reducing effect for sound propagating outdoors from traffic noise sources.
- [Yuan et al., 2019] Yuan, M., Yang, F., and Pang, Z. (2019). Deep subwavelength split ring neck acoustic resonator. *Results in Physics*, 13:102322.